Developmental Biology **207,** 86–106 (1999)
Article ID dbio.1998.9173, available online at http://www.idealibrary.com on IDEAL®

Morphogenesis of the *Caenorhabditis elegans* Male Tail Tip

Can Q. Nguyen,*[,1] David H. Hall,†[,1] Ying Yang,* and David H. A. Fitch*[,2]

**Department of Biology, New York University, New York, New York 10003; and †Center for C. elegans Anatomy, Department of Neuroscience, Kennedy Center, Albert Einstein College of Medicine, Bronx, New York 10461*

Using electron microscopy and immunofluorescent labeling of adherens junctions, we have reconstructed the changes in cell architecture and intercellular associations that occur during morphogenesis of the nematode male tail tip. During late postembryonic development, the *Caenorhabditis elegans* male tail is reshaped to form a copulatory structure. The most posterior hypodermal cells in the tail define a specialized, sexually dimorphic compartment in which cells fuse and retract in the male, changing their shape from a tapered cone to a blunt dome. Developmental profiles using electron microscopy and immunofluorescent staining suggest that cell fusions are initiated at or adjacent to adherens junctions. Anterior portions of the tail tip cells show the first evidence of retractions and fusions, consistent with our hypothesis that an anterior event triggers these morphogenetic events. Available mutations that interfere with morphogenesis implicate particular regulatory pathways and suggest loci at which evolutionary changes could have produced morphological diversity.

Key Words: **morphogenesis; *C. elegans;* adherens junctions; gap junctions; cell fusion; male tail; evolution.**

INTRODUCTION

How cells are coordinated to change their form remains a fundamental question in developmental biology. To understand the mechanisms and components underlying multicellular morphogenesis, we have begun a comprehensive study of the four-celled male tail tip of *Caenorhabditis elegans.* Cell fusion, changes in cell shape and position, fluid displacement, nuclear migration, and changes in intercellular associations are all important features of male tail tip morphogenesis, as they are in other systems. Cell fusion plays an important role in many steps of development in *C. elegans* (Podbilewicz and White, 1994; Newman *et al.,* 1996), in other invertebrates (Doberstein *et al.,* 1997; Tanaka-Matakatsu *et al.,* 1996), and in vertebrates (see Podbilewicz and White, 1994). In vertebrates and invertebrates, cell shape changes are important during embryogenesis in events like gastrulation or elongation and in forming an array of epithelial structures via folds or placodes (Priess and Hirsh, 1986; Kam *et al.,* 1991).

Morphogenesis occurs rapidly during the last larval (L4) stage to dramatically change the shape of the tail from a simple tapered cone to the complex morphology of the copulatory bursa or "male tail" (Figs. 1A–1F). General male tail morphogenesis and patterning of the male-specific sensilla ("ray" papillae) also involve a complex series of developmental events, including anteroposterior identity specification by the Hox gene complex, intercellular signaling, and hypodermal cell fusions (reviewed in Emmons and Sternberg, 1997). The first visible sign of male tail morphogenesis occurs when the cells in the tail tip become rounded and retract anteriorly (Fig. 1B). Here we focus on the dynamic cellular and subcellular changes in the architecture of the tail tip during this first step of male tail morphogenesis.

The lineages of the tail tip cells (hyp8–hyp11) are known and are the same for both sexes (Sulston and Horvitz, 1977; Sulston *et al.,* 1980, 1983). These hypodermal cells originate early in embryogenesis and adopt their characteristic tapered shapes when other hypodermal cells elongate dur-

[1] These two authors contributed equally.

[2] To whom correspondence should be addressed at Department of Biology, New York University, Room 1009 Main Building, 100 Washington Square East, New York, NY 10003. E-mail: david.fitch@nyu.edu.

0012-1606/99 $30.00

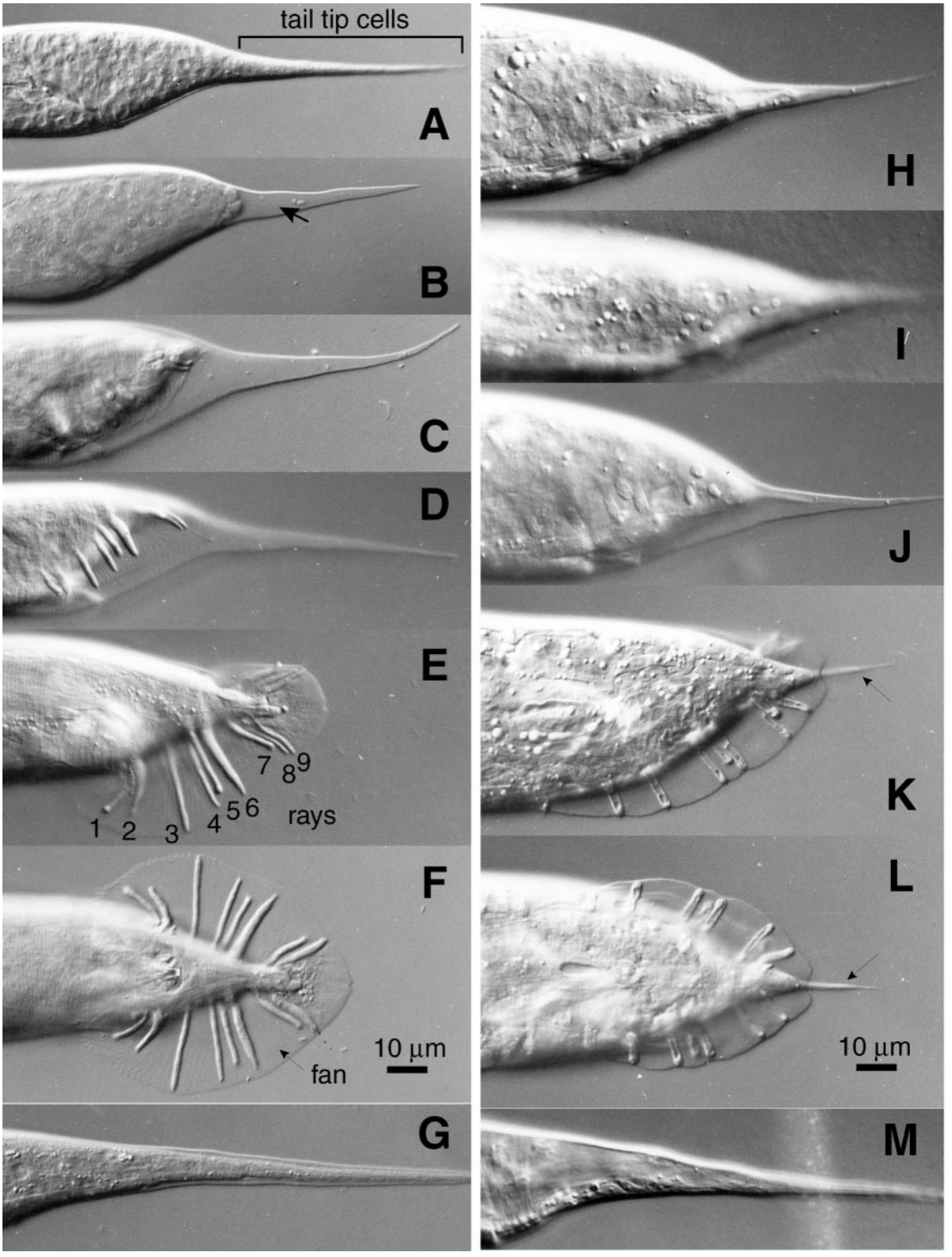

FIG. 1. Male tail morphogenesis in two species (anterior at left, lateral views, except ventral views in F and L). (A–F) Wild-type *C. elegans* male from late L3 (A) through L4 morphogenesis (B–D) to adulthood (E, F). (B) The arrow marks the extracellular space left in the wake of anteriorward retraction of the tail tip. (E) Side view of the "peloderan" adult male tail with rays (numbered). (G) The *C. elegans* hermaphrodite retains the pointed shape of the larval tail. Failure in tail tip retraction during male morphogenesis in *O. myriophila* (H–J) also results in a leptoderan adult tail (arrows in K and L). In *O. myriophila*, fluid still accumulates in the extracellular space while a leptoderan tail tip is maintained (J). (M) Adult hermaphrodite of *O. myriophila.*

ing midembryonic morphogenesis (Priess and Hirsh, 1986). The sexual dimorphism of the tail tip cells of adults (compare Figs. 1E and 1G) thus results not from differences in cell lineage, but from late postembryonic morphogenetic events specific to males.

Because *C. elegans* hermaphrodites are self-fertilizing and males are nonessential, genetic analysis of the male tail tip is greatly facilitated. Some mutations that disrupt tail tip morphogenesis are already available and are likely to lead us to the components and regulatory mechanisms underlying this process. However, a complete delineation of wild-type morphogenesis—undertaken here—is first required to provide a context for a meaningful analysis of mutant phenotypes.

Tail tip morphogenesis has changed during evolution. Within the nematode family Rhabditidae, which includes *C. elegans,* there is a surprising amount of morphological diversity for a structure with so few cells (Chitwood and Chitwood, 1950; Sudhaus, 1976). Tail tip morphology has classically been used to diagnose taxonomic levels as high as subfamilies (Andrássy, 1983). For example, the tail tip of *Oscheius myriophila* fails to retract during male morphogenesis (Figs. 1H–1J), resulting in a pointed ("leptoderan") tail tip that protrudes beyond the posterior edge of the adult fan (Figs. 1K and 1L). To reconstruct evolutionary changes resulting in this morphological diversity, a comprehensive understanding of the architecture of tail tip morphogenesis is first required.

To provide a detailed cellular foundation for understanding morphogenesis, we present an ultrastructural analysis of changes in cell–cell relationships during morphogenesis and identify key features that could underlie morphogenetic mechanisms: e.g., a posteriorward progression of cell fusions which are initiated at adherens junctions, sex-specific cell–cell contacts, gap junctions between hypodermal cells, and a system of vacuoles that could have been recruited for fluid transport. We have used serial thin-section reconstruction and immunofluorescence labeling of adherens junctions to identify structural bases for possible sites of cell fusions and cell–cell communication as well as the nature of the changes in cell shape and position that accompany tail tip morphogenesis. We have also used immunofluorescence to characterize a mutant and other species in which male tail tip morphogenesis specifically fails. These comparisons suggest that heterochronic delays in fusions and retraction can be effected by changes at a single locus and could have produced morphological diversity during evolution.

MATERIALS AND METHODS

Nematode Strains and Culture

Mixed stages of wild-type strains of *C. elegans,* N2 and CB4088 (Hodgkin *et al.,* 1979), were maintained separately at 20°C on NGM plates seeded with *Escherichia coli* OP50 (Brenner, 1974). CB4088 bears the mutation *him-5(e1490)V,* which confers a high incidence of males with normal tails (Hodgkin *et al.,* 1979). The *bx37* and *bx42* alleles of *lep-1* (strains EM101 and EM106) were generously provided by Dr. Scott Emmons (Albert Einstein College of Medicine). The EM435 strain of *O. myriophila* was described previously by Fitch and Emmons (1995) as "*Rhabditis* sp. *br.*" Details about the strains of *Rhabditella axei* (DF5006) and others are available from our web site (http://www.nyu.edu/projects/fitch/WSRN/). Another unidentified *Rhabditis* species was isolated from an earthworm in the Bronx, New York, and used for immunofluorescent labeling experiments; unfortunately, this strain has since been lost.

Mixed-stage populations containing mostly late (L3 and L4) larvae and adults were obtained by two alternative methods. (1) For immunohistochemistry, gravid adults were washed with M9 buffer (Brenner, 1974) and treated with alkaline hypochlorite as described by Sulston and Hodgkin (1988). (2) For electron microscopy (EM), gravid adults were placed on freshly seeded plates for several hours and allowed to lay eggs; adults were subsequently washed off. Both methods left synchronous populations of fertilized eggs to develop on plates at room temperature (20–22°C) until they reached late stages.

MH27 Immunofluorescence and Image Processing

Mixed-stage populations containing mostly late larvae were washed twice in M9 and fixed in 1% paraformaldehyde and MRWB (Finney and Ruvkun, 1990) during four to five freeze–thaw cycles over 30 min. Fixed worms were permeabilized by the "redox" method of Finney and Ruvkun (1990), incubated for 4–12 h at 37°C with a 1:100 dilution of monoclonal MH27 antibody (generously provided by R. Waterston, Washington University, St. Louis, MO), and incubated with a 1:50 dilution of goat serum and a 1:50 dilution of rhodamine-conjugated goat anti-mouse antibody (Boehringer-Mannheim Biochemicals) for 4–12 h at 37°C. Specimens were observed on a Zeiss Axioskop equipped for epifluorescence and photographed at several focal planes using Kodak TMax-400 film exposed for 15 s and push-processed two stops. Negatives were digitally scanned with a Nikon scanner. Using Adobe Photoshop, digital images of different focal planes for the same animal were layered together and contrast was enhanced.

Electron Microscopy

Mixed-stage populations of late larvae were washed with M9 buffer and fixed without anesthesia in 2.5% glutaraldehyde, 1% formaldehyde in 0.05 M Hepes at room temperature for 150 min (general methods have been reviewed by Hall, 1995). The tails were cut open immediately in the primary fixative to ensure good access to the tissue. After several buffer rinses, tails were fixed again in 1% osmium tetroxide in 0.1 M Hepes for 2 h at room temperature. After further rinses, tails were embedded in 2.5% SeaPlaque agarose (FMC Bioproducts) and stored overnight at 4°C under buffer. Postembedded tails were stained in 1% uranyl acetate for 1 h at room temperature, dehydrated, and embedded in Medcast resin (Ted Pella) for thin sectioning. Serial transverse thin sections (1000 per tail) were collected and poststained with alcoholic uranyl acetate and aqueous lead citrate before viewing with a Philips CM10 electron microscope. Selected sections were photographed.

Serial Section Reconstruction

The three-dimensional shapes and sizes of individual cells and organelles were reconstructed by tracing their outlines on a digi-

tizing pad using the RECON SSRS program (Sun Technologies, Raleigh, NC) running on a PC. Output from the SSRS package was plotted on an HP 7475 plotter to visualize cells as wireframe models at selected angles. Since the total cell volume calculations were sensitive to the precision of section thickness (which varied somewhat among animals), we report only the relative volumes calculated for the hyp cells in comparison to the total volume calculated for all four cells in each animal, disregarding any possible growth or shrinkage of the tail. There were no clear trends indicating hyp cell growth or shrinkage prior to normalization (not shown). The total volume of intracellular vacuoles is reported as a percentage of the cytoplasmic volume of the same cell (less the vacuole volume). Extracellular space is reported as a percentage of the combined volumes of the four hyp cells.

RESULTS

C. elegans male tail morphogenesis begins immediately after completion of the cell divisions that form the bursal papillae or "rays" (Fig. 1). The tail tip cells then lose adhesion with the larval cuticle and recede anteriorly, leaving behind a clear fluid in the extracellular space (arrow, Fig. 1B). Because of this retraction of the tail tip, the adult male tail is blunt ended and "peloderan" (i.e., the bursa velum or "fan" extends posteriorly and envelopes the blunt tail tip; Figs. 1E and 1F). As tail tip retraction occurs, other cells in the male tail (e.g., ray cells) alter their contacts, shapes, and positions (Sulston *et al.*, 1980; Baird *et al.*, 1991). These events are not visible at the gross morphological level until after the tail tip cells retract, when the ray papillae become visible on the lateral surface (Figs. 1C and 1D; see also Baird *et al.*, 1991). The pointed hermaphrodite tail tip results from a retention of the larval form as no major morphogenetic change occurs (Fig. 1G).

Tail Tip Cell Neighbors Are Sexually Dimorphic before the Tail Tip Cells Become Sexually Dimorphic

The sexual dimorphism between the tail tips of hermaphrodites and males could be prefigured by a structural difference in the tail tip cells themselves prior to male-specific morphogenesis. As detailed below, however, the only sexual differences involve neighboring cells, not the tail tip hypodermal cells themselves. To reconstruct the three-dimensional arrangements of the tail tip cells with respect to each other and their neighbors, we studied EM images of serially sectioned adult hermaphrodite tails and L4 male tails. Due to their small size and intricate folding, EM proved essential for reconstructing tail tip cell shapes and arrangements.

The hermaphrodite tail tip. In the hermaphrodite tail tip (as in the male, discussed later), three of the four tail tip hypodermal cells (hyp8, hyp9, and hyp10) are organized in telescopic fashion, such that each succeeding cell fits into the next most anterior cell (schematized in Fig. 2A). This interlocking organization may allow flexibility of the tail tip such that each cell can rotate against its neighbor without tearing the zone of contact. The nuclei lie near the anterior end of each cell, within the anal hypodermal ridge (a large ridge of hypodermal tissue beneath the basal lamina, the anterior portion of which stretches dorsally over the rectum, terminating at the dorsorectal ganglion). The most posterior cell, hyp10, contains two nuclei due to a cell fusion during embryogenesis (Sulston *et al.*, 1983). The most anterior and dorsal cell, hyp11, lies as a half-cylindrical projection, draped over the anal ridge and separated by a basal lamina from the ridge itself (Fig. 2). The basal lamina may allow apposing cells to slide past each other, also contributing to the flexibility of the whip-like tail. The nucleus of hyp11 is asymmetrically located on the left side; this cell also has a narrow arm that reaches anteriorly along the left side of the body wall (Fig. 2A). The apical borders of the hypodermal cells are characterized by a continuous band of adherens junction (*zonula adherens*) where these cells touch the body wall (represented in red in Fig. 2). Adherens junctions were observed both in electron micrographs and by immunofluorescent staining with a monoclonal antibody, MH27, that recognizes an epitope in these junctions (discussed later). We observed that several neuronal processes (including several sensory dendrites) extend into the extreme tip of the tail and appear to be closely associated with the posterior hypodermal cells (Hall, 1977; Hall and Russell, 1991). Several of these processes (PVR, PDB, and especially the PHCs) fit into small channels that penetrate the hypodermal cells (most notably hyp10) with direct membrane–membrane contacts; most (i.e., PLMs, PLNs, PVR, PDB, and PHCs) run in close association with hyp8 and/or hyp9, but are generally separated by basal lamina (Fig. 2B, Table 1A). Some of the cells supporting the phasmid chemoreceptor also contact the tail tip cells. The most anterior two cells, hyp8 and hyp11, additionally contact the main body hypodermis, a large syncytium called hyp7 (Fig. 2, Table 1A). In hermaphrodites, these cellular arrangements and contacts persist from postembryonic development through adulthood.

The male tail tip. In both EM reconstructions and MH27 staining, we found that the arrangement of the tail tip hypodermal cells (hyp8–hyp11) in larval males prior to morphogenesis is similar to that in hermaphrodites, except for contacts made with male-specific cells (Fig. 3, Table 1B). One such sexual difference involves a syncytium that contacts hyp8 and contains two ventral hypodermal nuclei [with nuclear lineages AB.p[l/r]appppa (i.e., sisters of the T cells); see Sulston *et al.*, 1983, for cell lineage nomenclature]. Although the nuclei are the same in males and hermaphrodites, we found them in hermaphrodites within the main body syncytium, hyp7, but in males in a previously undescribed, separate, binucleate cell that we call "hyp13" (Fig. 3D, Fig. 4). Because the apical surface of hyp13 is surrounded by adherens junctions, hyp13 can be visualized by MH27 staining. hyp13 can be used empirically to differentiate males from hermaphrodites from at least the L2 stage (not shown; L1s and embryos were not

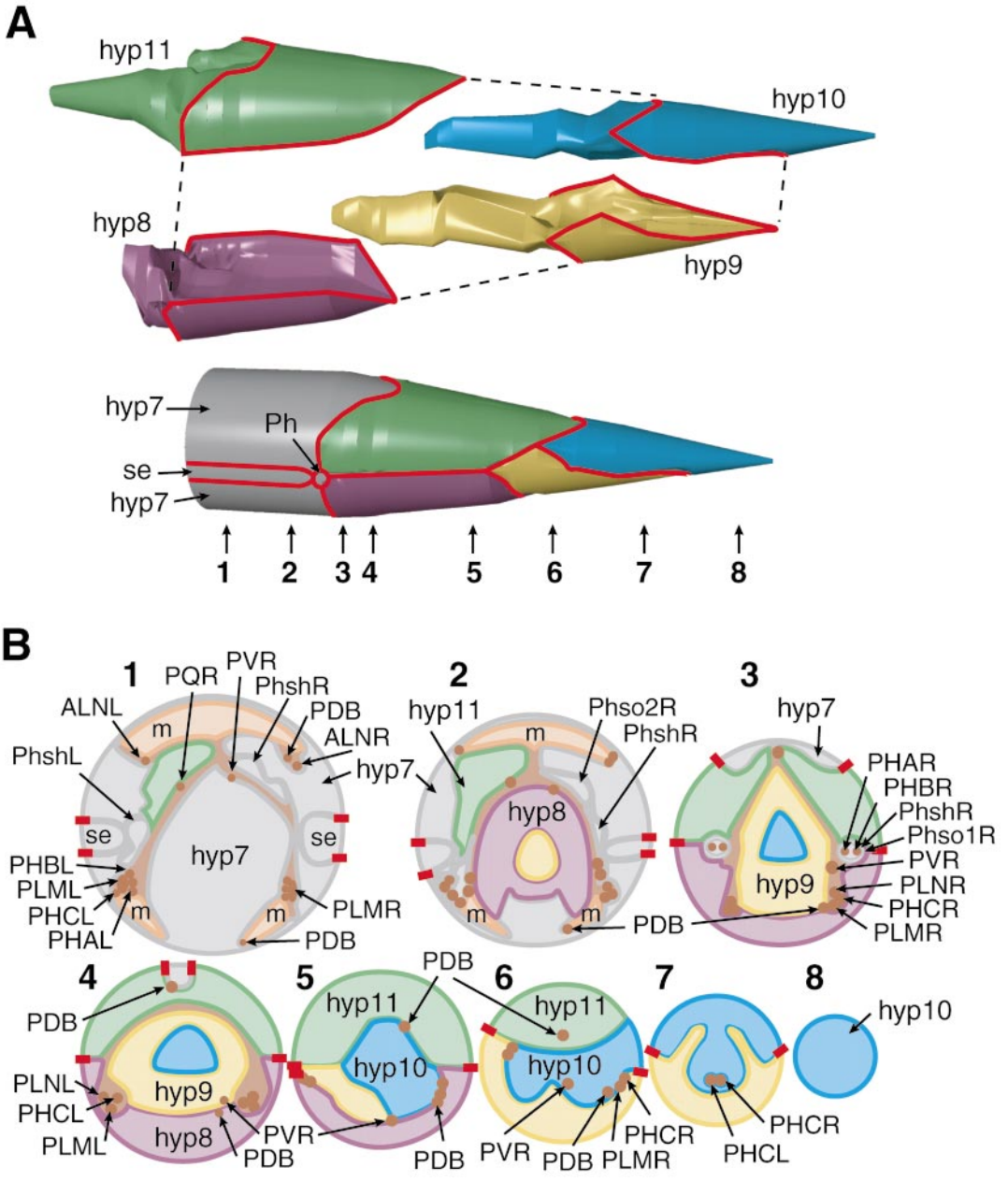

FIG. 2. Three-dimensional arrangement of the tail tip hypodermal cells in the *C. elegans* hermaphrodite. This schematic model is deformed (made shorter along the anteroposterior axis) to fit the page; actual tails are quite elongated (cf. Fig. 1G). The four color-coded hypodermal cells are shown separated in an "exploded" view and together as they would normally appear in the conical tail tip (A); hyp10 (cyan) fits into hyp9 (gold), which penetrates hyp8 (purple); hyp11 (green) fits on top. Anterior is left, ventral down. Red lines indicate the adherens junctions which contiguously mark the cell borders at the body wall. Also depicted are the main body syncytium (hyp7), lateral seam (se), and phasmid socket (Ph). Eight transverse sections from the points indicated by the numbered arrows are also schematized (B). Schematized sections 1–8 are abstracted from thin sections (from anterior to posterior, respectively, 172, 259, 346, 376, 481, 595, 900, and 1231 of 1600 total) from an adult hermaphrodite series (B116). The hypodermal cells are color coded as in A: body wall muscle (m) is light orange, basal lamina is beige, neuronal dendrites are brown dots (named as in White, 1988; see Table 1), and other cells are gray. Red rectangles represent adherens junctions. The dendrite of PDB loops back at section 600.

tested). hyp13 fuses with hyp7 only at the very end of male morphogenesis.

We observed another sexual difference that involves the cells contacting the anteriorly projecting left arm of hyp11. As in hermaphrodites, this arm was consistently found in eight reconstructed male tails (e.g., Figs. 3C and 3D). In one

TABLE 1
Cell Contacts of Tail Tip Hypodermal Cells

Cells contacted	Type of contact with tail tip hyp cell[a]			
	hyp10	hyp9	hyp11	hyp8
A. In L4 and adult hermaphrodites				
hyp9	aj, gj	—	—	—
hyp11	aj, gj, bl	aj, bl	—	—
hyp8	nc/gj	aj, gj, bl	aj, gj, bl	—
hyp7	nc	nc	aj, gj, bl	aj, gj, bl
PLMs[b]	bl	bl	nc/bl	bl
PLNs[b]	bl	pm	pm	pm
PVR[c]	pm	pm	pm	pm
PDB	pm	pm	pm	pm
PHCs[b]	bl, pm	pm	pm	bl
Phsh (phasmid sheath cells)[b]	nc	nc	pm/nc	pm
Phso1 (primary phasmid socket cells)[b]	nc	bl	aj	aj
Phso2 (secondary phasmid socket cells)[b]	bl/nc	bl/nc	pm	pm/bl
Dorsal body wall muscles	nc/close	nc/close	bl	nc
Ventral body wall muscle	nc	nc	nc	bl
B. In early L4 males prior to ray cell morphogenesis				
hyp9	aj, gj	—	—	—
hyp11	aj, gj, bl	aj, bl	—	—
hyp8	nc/gj/bl	aj, gj	aj, gj, bl	—
hyp7	nc	nc	aj, gj, bl	nc
hyp13	nc	nc	nc	aj, gj
ALNL	nc	nc	nc/pm	nc
PVNL	nc	nc	nc/pm	nc
PLMs[b]	bl, pm	bl, pm	bl	bl
PLNs[b]	nc	bl	pm	pm
PVR[c]	nc	nc	pm/nc	nc
PDB	bl, pm	bl	bl, pm	bl
PHCs[b]	bl	bl	bl	bl
Phsh (phasmid sheath cells)[b]	nc	nc	nc/pm	bl, pm
Phso1 (primary phasmid socket cells)[b]	nc	bl	aj, pm/bl	aj
Phso2 (secondary phasmid socket cells)[b]	nc	bl/close	aj/pm[d]/bl/close	bl/close
Dorsal body wall muscle	nc	nc	bl	nc
ventral body wall muscle[b]	nc	nc	nc	bl
R9st (ray 9 structural cell)[b]	nc	nc	pm/bl/nc	nc
R9.p[b]	nc	nc	aj, pm	nc
R9A (ray 9 type A neuron)[b]	nc	nc	pm/bl/nc	nc
R9B (ray 9 type B neuron)[b]	nc	nc	pm/nc/bl	nc
R8st[b]	nc	nc	pm/nc/bl	nc
R8.p[b]	nc	nc	pm/aj/bl/nc	pm/aj[e]
R8A[b]	nc	nc	nc	nc
R8B[b]	nc	nc	nc/bl	nc
R7st[b]	nc	nc	nc/pm	nc
R7.p[b]	nc	nc	nc/pm	nc
R7A[b]	nc	nc	nc	nc
R7B[b]	nc	nc	nc	nc

[a] Cell contacts occur via gap junctions (gj) or adherens junctions (aj) in addition to direct contact between plasma membranes or direct contact only occurs between plasma membranes without specialized contacts evident (pm). Cells may also be closely apposed across a basal lamina (bl). Some cells do not touch directly but are in close proximity to each other (close). Several cells never contact each other (nc). A slash (/) indicates variation among individual animals.

[b] These cells occur as bilateral pairs; e.g., the PLMs are PLML on the left and PLMR on the right.

[c] Because the PVR dendrite is not always present in the tail tip, the contacts it makes with the tail tip cells are variable. When present, it crosses from the right side to the anal ridge where it appears across the basal lamina from hyp11 or it penetrates the basal lamina and becomes embedded into hyp11.

[d] The soma of the Phso2L cell is sometimes contacted by hyp11 (pm).

[e] Although hyp8 usually does not appear to contact R8.p at the body wall at early L4 stages, these cells are usually joined by adherens junctions later when ray cells cluster together.

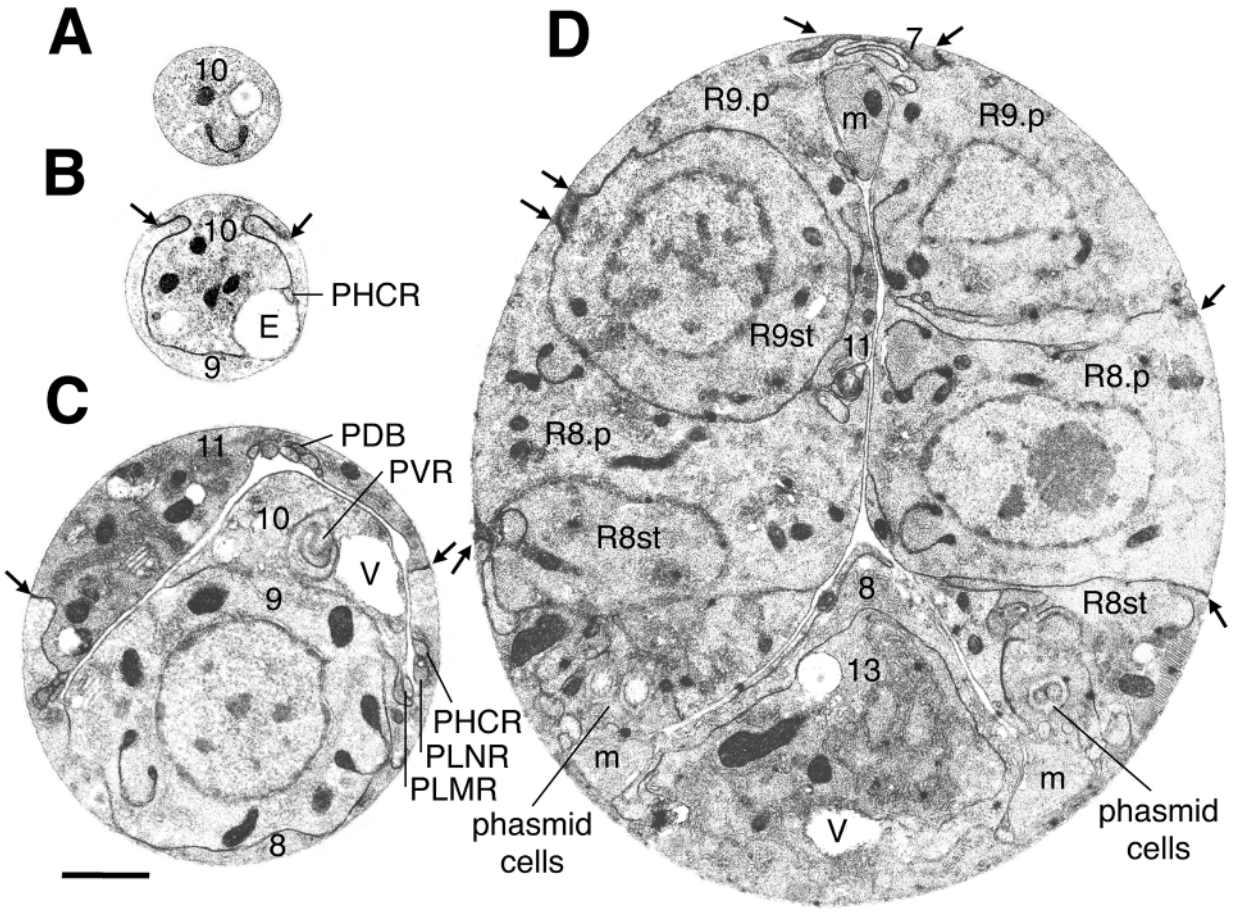

FIG. 3. Sample thin sections (A–D, posterior to anterior) from a stage 0 male demonstrate the initial relationships (before fusion or retraction) of the tail tip cells with neurons, muscles (m), and other hypodermal cells. Hypodermal cells are labeled by number (8, hyp8; 9, hyp9; 10, hyp10; 11, hyp11; 13, hyp13). Other cells are labeled as in Table 1 and Fig. 2. Short arrows indicate sites of adherens junctions. Cell arrangements are very similar to those in the mature hermaphrodite tail (cf. Fig. 2), except that male-specific cells (bilateral pairs of R9.p, R9st, R8.p, and R8st) are present. In D, for example, hyp11 makes plasma membrane contacts with R9st and R9.p on the left side. On its right side, hyp11 also touches basal lamina. There is early evidence of vacuole production (V) and expansion of extracellular space (E). Scale bar, 1 μm.

reconstructed male animal the nucleus and the anterior arm of hyp11 were on the right side, apparently due to a mirror reversal of the body plan (not shown; cf. Wood, 1991). Although in hermaphrodites hyp7 is the only hypodermal cell that is contacted by this hyp11 arm, in males this arm contacts several male-specific cells (Fig. 3D; Table 1B), of which R9.p and sometimes R8.p contact hyp11 at adherens junctions (Figs. 4A and 4B; Table 1B). At the apical surfaces of these cells, these contacts are mediated by adherens junctions and are easily visualized by MH27 staining (Table 1B; Fig. 4A, represented by red lines in Fig. 4B). R9.p and R8.p are posterior sisters of cells that are progenitors of the ray neurons and support cells. The male-specific lineages that produce these cells begin during the late L3 stage and continue through mid-L4 (Sulston *et al.*, 1980). Thus, the only structural differences in larval tail tips between the sexes appear to involve the neighbors of the tail tip hyp cells; the tail tip cells themselves are identical.

Adherens and Gap Junctions Link the Hypodermal Cells

We closely inspected the boundaries of the tail tip cells to analyze the distribution of adherens and gap junctions using high-magnification prints (ca. 30,000×) (e.g., Figs. 5A and 5B). Adherens junctions were also visualized by immunofluorescent staining with MH27 antibody ($N > 100$; Fig. 4); the resulting staining patterns conformed exactly to those expected from the electron micrographs. MH27 has been shown previously to bind adherens junctions by immunocytochemistry (Hall, 1996). Specifically, the apical borders

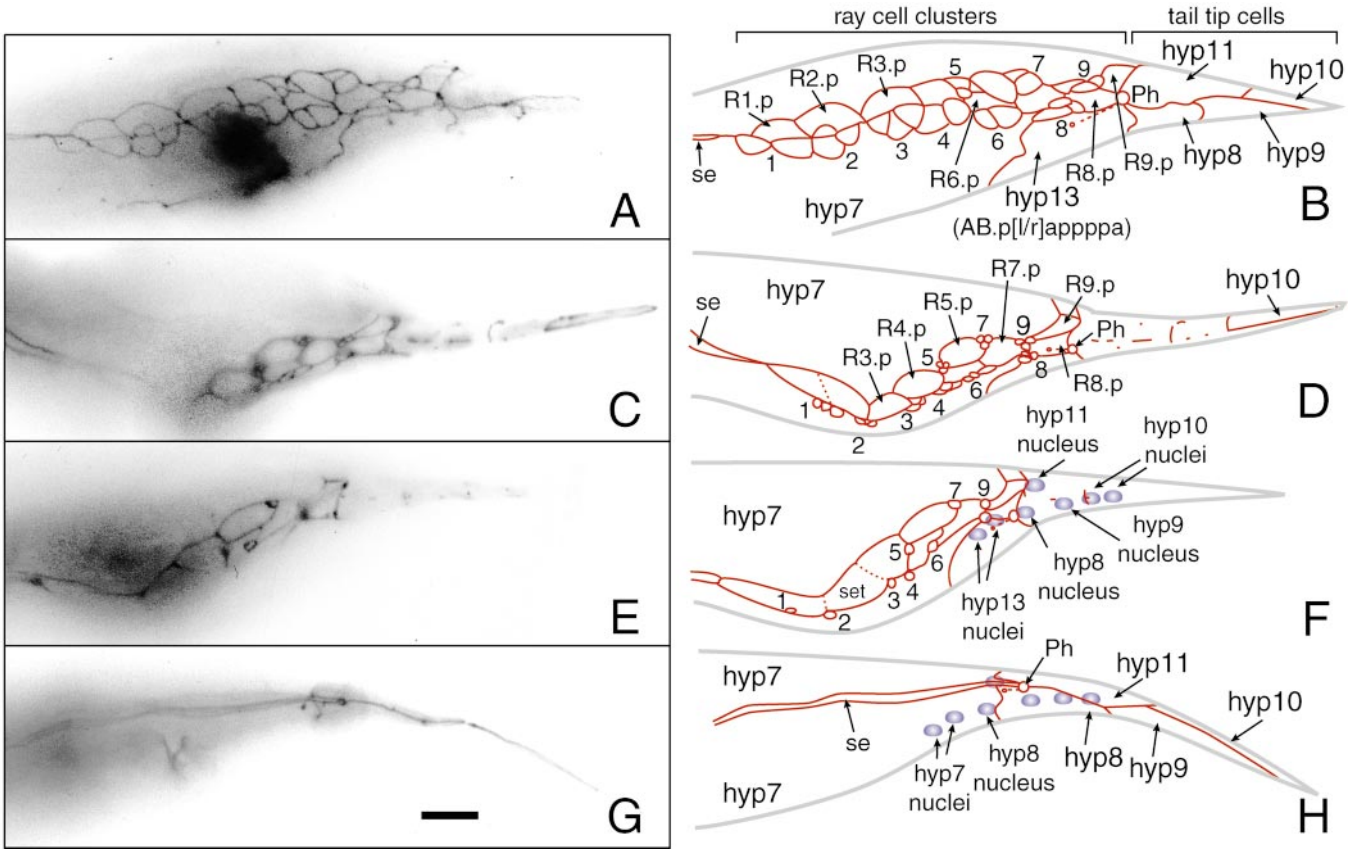

FIG. 4. Early stages in wild-type male tail development, prior to tail tip retraction (A–F), and a late L4 hermaphrodite tail (G, H), viewed by MH27 immunofluorescent staining. Scale bar, 10 μm. (A, C, E) Immunofluorescence images (negatives) of MH27 staining at three successive stages during L4 male development. (B, D, F, H) Tracings of the MH27 staining (red lines) shown in A, C, E, and G, respectively. Until the mid-L4 stage, the tail tip hyp cells (hyp8–hyp11), phasmid (Ph), and lateral "seam" hypodermis (se) are arranged similarly between the sexes. Male-specific cells include the ray cell clusters (numbered) and the hyp13 compartment (which fuses with the hyp7 syncytium in hermaphrodites before L2 or earlier, but only at very late L4 in males). Cell borders show fragmented staining as cell fusion progresses (D, F). The tail tip cells do not fuse in hermaphrodites; arrangements of cells in the adult hermaphrodite tail are similar to those shown (G, H). Positions of the hyp cell nuclei are shown as blue ovals (determined from DAPI costaining). Each cluster of cells that will differentiate to form a ray is numbered (1–9). During male development, the two cells from each ray cell cluster that will become ray neurons sink slightly away from the body wall, leaving a small circle of MH27 staining at the surface corresponding to the ray structural cell (R*n*st; numbered 1–9 in F), while the exterior face of each Rn.p hypodermal cell enlarges. Some of these Rn.p cells fuse (dashed lines), beginning with the anterior cells, to form the tail seam ("set") syncytium along the lateral margin (F). There is little variation in relative timing between the ray cell and the tail tip cell morphogenetic events.

of all hypodermal cells are bordered by adherens junctions where these cells touch the body wall (Fig. 5A).

Many adherens junctions are distributed similarly in hermaphrodites and larval males; e.g., around the tail tip cells hyp8–hyp11, hyp7, the lateral seam (se) cells, and the primary phasmid socket (Phsol) cells (see Table 1). However, the male-specific hyp13 compartment and cells derived from the ray lineages form adherens-mediated contacts that are not present in hermaphrodites (compare parts A and B of Table 1 and Figs. 4A and 4B with Figs. 4G and 4H). In males, adherens junctions remain intact until the time of hyp cell fusions (discussed later).

By closely examining the tail tip hyp cells, we also uncovered an extensive series of electrical synapses, or gap junctions, connecting these cells to their neighbors (Fig. 5B). In hermaphrodites, gap junctions are common between hypodermal cells in the tail and elsewhere (Table 1A; Hall, 1987 and unpublished; White, 1988) and permit the intercellular transfer of small molecules from embryogenesis through adulthood (Bossinger and Schierenberg, 1992; Starich *et al.*, 1996). A similar distribution of gap junctions is found between female and male tail tips before the onset of tail tip morphogenesis (Table 1B).

We did not find these specialized junctions at all areas of cell–cell contact. For example, hypodermal cells may contact other cells over extensive distances where there are no

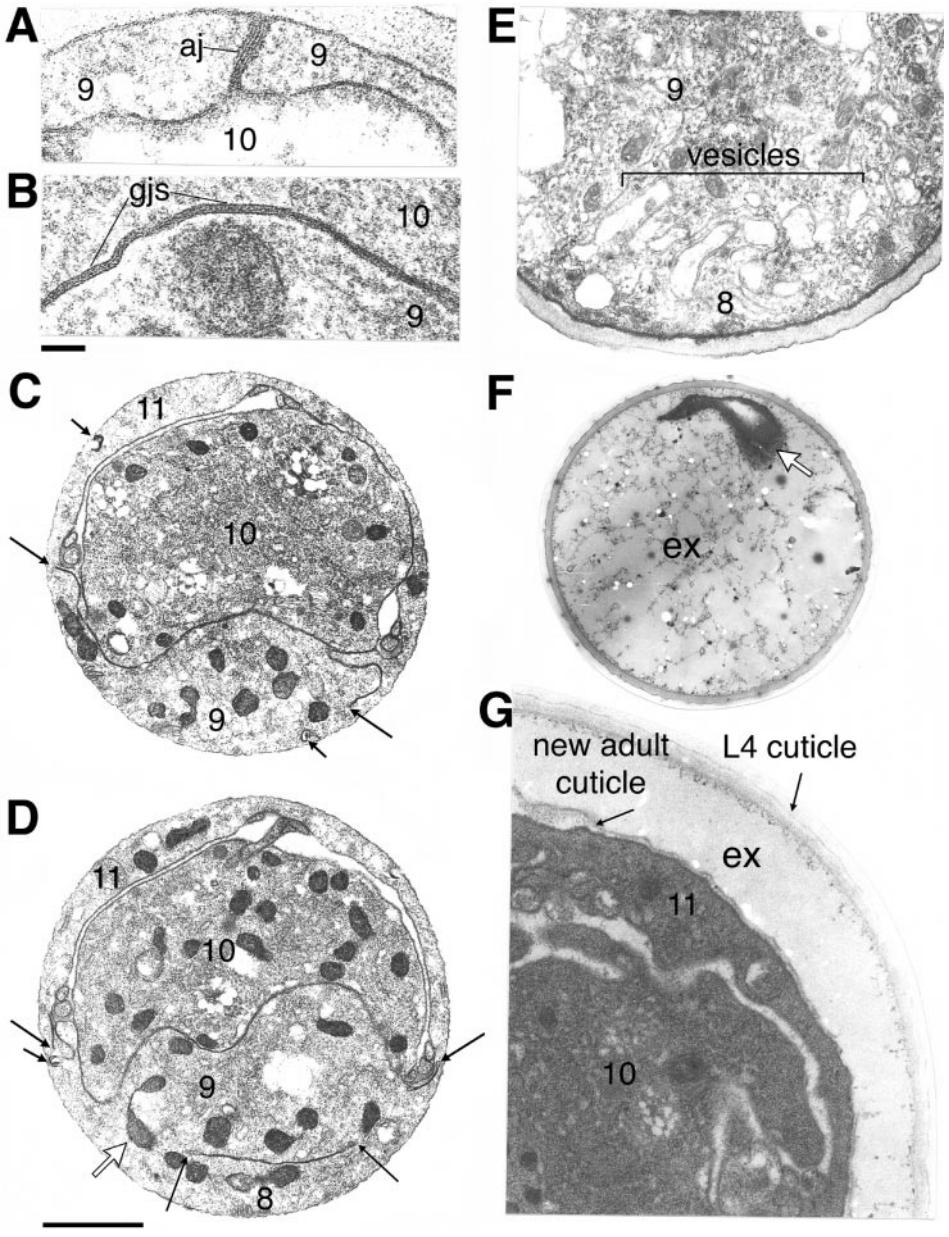

FIG. 5. Ultrastructural features of cell junctions, cell fusions, and tail tip retraction in sample electron micrographs from serially sectioned male tails. Hypodermal cells are labeled by number as in Fig. 3. (A) An adherens junction (aj) that seals hyp9 to itself in the very posterior portion of the tail tip. (B) Gap junctions (gjs) between hyp9 and hyp10. Scale bar, 10 nm for A and B. Fusions are initiated as "breaks" in the plasma membranes that tend to be closer to the body wall in posterior (C) than in anterior (D) sections, suggesting that the fusions began anteriorly and "zippered" posteriorward (scale bar, 1 μm for C–E and G, but 0.5 μm for F). Short arrows mark curled membrane/adherens remnants. Long arrows indicate remaining "broken" edges of membrane near presumptive sites of fusion. A mitochondrion spans the fused hyp cells (open arrow, D). (E) In one stage 3 male where fusions were completed, a collection of membranous vesicles accumulated near the former boundary between hyp8 and hyp9. (F) During retraction, the larval cuticle in a stage 3 animal surrounds much extracellular space (ex) at the tail tip with only a remnant of hyp10 tissue (arrow). (G) More anteriorly, increased extracellular space primarily lies between old and new cuticle layers, whereas the space between cells remains small.

adherens junctions (e.g., between hyp10 and hyp9 in Fig. 3C; between hyp8 and hyp13 in Fig. 3D). Also, gap junctions have not yet been found between hyp9 and hyp11. Some tail tip hyp cells may not always maintain direct contact. For example, hyp8 and hyp10 often do not touch but sometimes contact each other via gap junctions or are apposed across

basal lamina. Although each tail tip hyp cell may not be directly linked to every other hyp cell ("in parallel"), the four cells in this "tail tip compartment" are all linked together through at least one other hyp cell ("in series").

Temporal Analysis of Male Tail Tip Morphogenesis

Using MH27 staining of adherens junctions ($N > 100$) in conjunction with serial thin section analysis ($N = 9$), we have delineated stages of male tail tip morphogenesis. Although MH27 staining cannot display all cell contacts, it has been extremely useful in monitoring changes in relative cell positions and cell fusions during morphogenesis (Francis and Waterston, 1985; Baird *et al.*, 1991; Podbiliwicz and White, 1994; Fitch and Emmons, 1995) and allows observations of large numbers of fixed animals. To provide landmarks for predicting the relative timing of tail tip events, we used states of differentiation of the ray cell groups (coincident with tail tip morphogenesis within a small margin of variation) as follows [note that these "stages" of tail tip morphogenesis do not correspond to the stages of ray cell morphogenesis defined by Fitch and Emmons (1995) which cover a broader temporal range].

At a time point that we call "stage 0" (Figs. 4A and 4B), the tail tip remains completely unretracted (see also Fig. 1A). Early ray cell progenitors occupy large territories along the body wall. Several of the more posterior ray cell progenitors form adherens junctions directly with tail tip hyp cells ("aj" contacts in Table 1B). Note also that the hyp13 syncytium contacts hyp8 via adherens junctions. The same arrangements of apical cell surfaces and adherens junctions at this stage were noted by EM ($N = 1$; Fig. 3). Progression from stage 0 through the following stages (to "stage 3") occurs from mid-L4 to late L4 and takes about 2.5 h at 20 ± 2°C.

By "stage 1" (Figs. 4C and 4D), the territories of the developing ray cells along the body wall begin to constrict to very small patches as viewed by MH27 staining, whereas the territories of the R*n*.p hypodermal cells expand somewhat on the body wall. R1.p and R2.p have often fused by this time. By EM ($N = 2$), however, the ray cell precursors show little differentiation at this stage. In the tail tip, hyp cell fusions begin to appear as punctate losses of MH27 staining at the hyp cell borders and progress from anterior to posterior: hyp8 and hyp11 fuse first, followed by fusions with hyp9 and finally hyp10. Fusions were also observed in EM serial sections as small breaks in the plasma membrane at the adherens junctions (Figs. 5C and 5D; described later).

By "stage 2" (Figs. 4E and 4F) the dendrite of each ray neuron begins to narrow and its soma sinks away from the lateral surface and is encircled by the tubular structural cell, which remains attached to the body wall by robust adherens junctions. R1.p–R5.p are in the process of fusing at this time to form the "tail seam" ("set"; Fig. 4F). As additionally observed by EM ($N = 3$), distal portions of the ray cells begin to form rudimentary dendritic specializations. Adherens junctions between the four tail tip hyp cells are almost completely gone by this stage, corresponding with EM observations. Positions of the nuclei have not changed significantly from their original positions.

By stage 3, each neuronal ray cell soma continues to sink away from the body wall, while its apical dendrite forms a small cilium attached to the body wall. As observed by EM ($N = 2$), fusions between the tail tip hyp cells are complete. The posterior hyp cells lose adherence with the L4 cuticle and begin to retract, leaving the characteristic fluid-filled extracellular space at the tail tip (Figs. 1B and 5F). By this stage, the nuclei of the hyp cells have begun their anteriorward migration. Retraction then proceeds rapidly to pull the rest of the cells anteriorward as the tail changes shape dramatically. In one animal, partial retraction of the tail tip was initiated prior to fluid expulsion, causing the distal portion of the tail spike to shorten and warp (not shown).

During retraction, some of the caudal dendrites that extend into the larval tail tip are gradually withdrawn anteriorly, although they are still present at stage 3. Eventually, some tail sense cells (PLM, PHC, and others) must resorb all or most of their posterior dendrites. The PLM cells retain only their anterior dendrite in the adult male. After retraction of the tail tip, many of these somata lie so caudal that there is no room to extend a posterior process. The caudal processes of the phasmid neurons are not lost, but are deflected to ventrolateral positions, still posterior to their somata.

Cell Fusions in Male Tail Tip Morphogenesis Initiate at or near Adherens Junctions and Progress from Anterior to Posterior

During stages 1 and 2, the fusions between the tail tip hyp cells occur at or adjacent to the adherens junctions. No additional specialized cytoplasmic structures are aligned with any of these junctions that would prefigure fusion events, in contrast to the prefusion vesicles required for *Drosophila* myotube fusion (Geiger *et al.*, 1995; Doberstein *et al.*, 1997). Fusions in the male tail result in a topological recombination of the plasma membranes between adjacent cells. One product of this fusion is a conjoined apical membrane bilayer (which thus surrounds both cells); the other product is a conjoined double bilayer at the former surfaces of contact between the cells. This latter conjoined double-bilayer product is detached from the body wall (long arrows in Figs. 5C and 5D) and internalized. Tiny segments of membrane remaining at the body wall (apparently containing vestiges of darkly staining adherens material) often form short curls (short arrows in Figs. 5C and 5D) which may drift away from the former anchorage site. Thereafter, the adherens junctions themselves (and the MH27 epitope) disappear completely (Figs. 4C–4F). Thus, we find a strong spatial correlation between sites of fusion and the adherens junctions. Although gap junctions are sometimes found near fusion sites (i.e., are near the conjoined "edges" of the internalized plasma membranes), they are also distributed

throughout these membranes where breaks have not occurred. Perhaps because of these gap junctions, the internalized membranes remain "pressed together" for a while.

Fusions appear to occur in a wave from anterior to posterior. By both EM and MH27 staining, we find that most early fusions occur between hyp9 and hyp11 (Figs. 5C and 5D) and between hyp8 and hyp11 (Fig. 5D); hyp10 is invariably the last cell to fuse (Fig. 4D). The internalized plasma membranes in the anterior portions of the cells have generally retreated further from the body wall (open arrow in Fig. 5D) than those in the posterior portions, which can still be attached to adherens junctions (or are at least closer to the body wall where adherens junctions have disappeared) (the internalized double bilayer may retreat from the body wall as a result of its elasticity). This topology suggests that fusions may occur by "zippering" in a posterior direction along the adherens junctions.

Fusions are essentially complete by stage 3, although excess membrane products persist for a short time. In at least one case, the aftermath of fusion was marked by a localized accumulation of many membranous vesicles, presumably preliminary products of membrane turnover (Fig. 5E).

Cell Shapes and Nuclear Positions Are Generally Stable until Fusions Occur

By MH27 staining ($N > 100$), the beginning of tail tip retraction does not appear to occur until after fusion initiation. However, details of individual cell shapes are not easily distinguished by this method. By tracing the outlines of cells in serial sections of staged male tails (as in Fig. 6), we have confirmed that the shapes of at least hyp9 and hyp10 are practically invariant among animals in stages 0–2 when fusions are initiated and completed (cells of a stage 0 male are shown in Figs. 6A, 6C, 6E, and 6G). Positions of all the nuclei remain stable throughout stages 0–2 (Table 2).

The earliest evidence for change in cell shapes (but without substantial change in nuclear position) was observed in one stage 1 male (Figs. 6B and 6D). In this animal, the anterior arm of hyp11 is enlarged, suggesting that the cell's volume is in the process of translocating rostrally along the arm itself (compare Fig. 6B to 6A). Similarly, the volume of hyp8 in this animal is subtly more rostral (Fig. 6D) than in an animal at an earlier stage (Fig. 6C). No fusions are observed in this particular animal, suggesting that initiation of retraction does not depend on fusion.

Evidence for retraction of the tail tip hyp tissues is always noticeable in stage 3, when fusions are essentially complete. In the wake of the anteriorward retraction of the hyp tissue, the extracellular space within the tail spike enlarges due to the accumulation of fluid (Fig. 1B and Figs. 5F and 5G). Because of the extensive fusion of hypodermal cell borders during stage 3, it was not usually possible to reconstruct their individual outlines as retraction progressed. However, in one stage 3 animal with hyp10 and hyp9 cell borders that could still be reconstructed by extrapolation of fusing membranes, there was substantial change in cell shape (compare Figs. 6F and 6H to Figs. 6E and 6G).

The nuclei of all four tail tip cells begin to move rapidly anteriorward in stage 3, concomitant with the hyp9 and hyp10 retractions (Table 2). These nuclear translocations are also observed by staining a population of fixed animals with DAPI (not shown) and have been observed previously (Sulston *et al.*, 1980), though are not documented at this fine a level of resolution. Interestingly, tail tip nuclei in hermaphrodites may also translocate somewhat anteriorly (Table 2). However, these translocations are not associated with cell shape changes and are not as extensive as in males. The nuclei in L4 males continue their anterior migrations far beyond where they stop in adult hermaphrodites.

Vacuoles May Shuttle Fluid through the Tail Tip to the Extracellular Space during Retraction

Although there is little change in the volumes of individual tail tip hypodermal cells relative to each other during male morphogenesis, there is a local swelling of intracellular vacuoles (denoted "V" in Figs. 3C and 3D). Vacuolar swellings are transitory and somewhat asynchronous, so one hypodermal cell may show pronounced vacuolar swelling in one specimen while a different hypodermal cell will be swollen with vacuoles in another individual (Table 3). At stage 0, the male tail hypodermal cells show a few cytoplasmic vacuoles (Figs. 3C and 3D), similar to those in an L4 hermaphrodite (not shown). During stages 1–2 of male tail morphogenesis, these vacuoles show a transient increase in volume, but by stage 3 they are greatly diminished. The relative amount of extracellular space is initially small (Fig. 3, Table 3), but suddenly increases at stage 3, particularly in the extreme tail tip (Figs. 5F and 5G; cf. Figs. 1A and 1B). Concomitantly, the degree of vacuolation dramatically decreases in hyp8, hyp9, and hyp11. We hypothesize that the hyp cells extrude the contents of these vacuoles around the time retraction is initiated.

Genetic Changes Can Alter the Relative Timing of Morphogenetic Events

We have characterized the progression of hyp cell fusions in males bearing mutations (*bx37* and *bx42*) in the locus *lep-1*. These mutations were originally isolated in the laboratory of Dr. Scott Emmons (Albert Einstein College of Medicine) in an F2 screen for male tail morphological defects using Nomarski microscopy. Tail tip retraction fails during L4 male morphogenesis (Figs. 7A–7D) in nearly all males that bear either of the hypomorphic mutations at the *lep-1* locus (Y.Y. and D.H.A.F., unpublished), resulting in leptoderan tail tips of variable size in adult males (Figs. 7E and 7F). However, the *lep-1* mutations do not affect morphogenesis of the fan and rays, suggesting that tail tip retraction is independent of general male tail retraction.

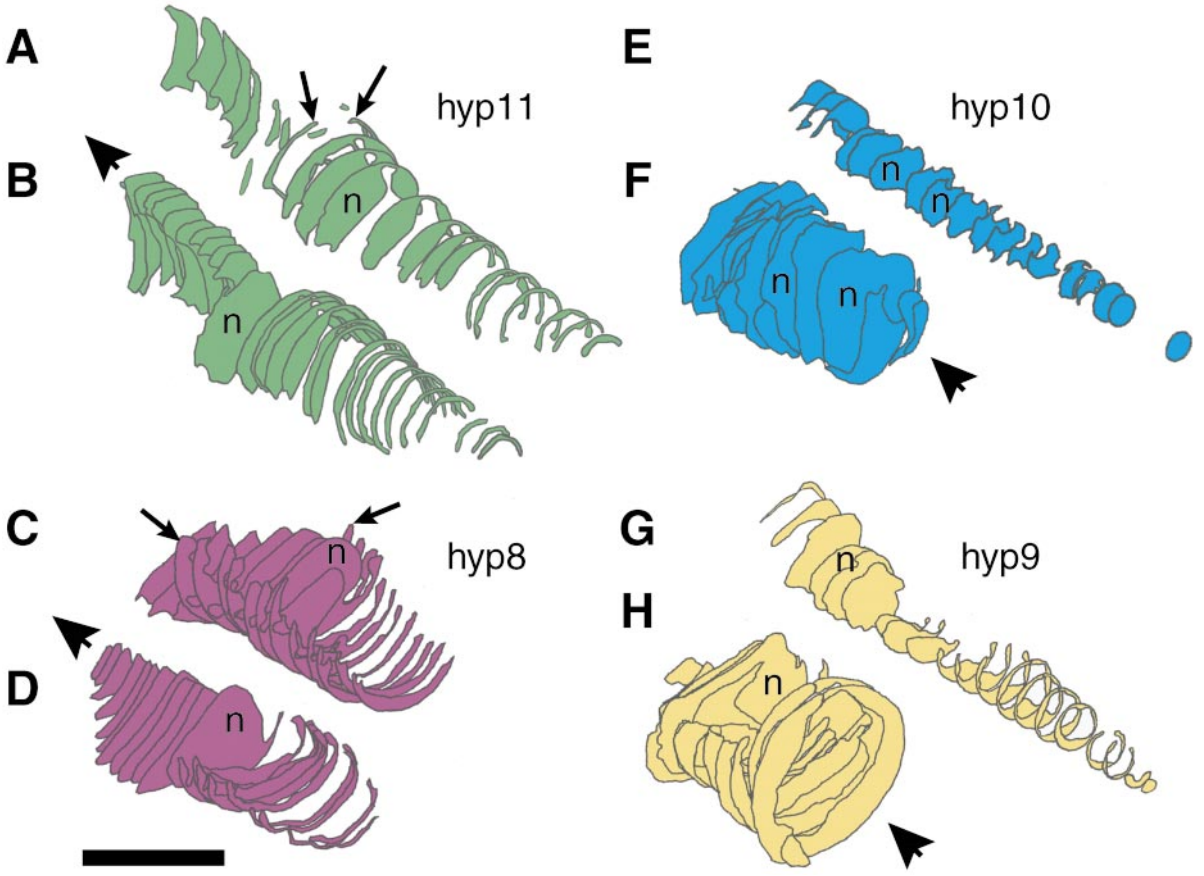

FIG. 6. Changes in cell shape begin with anterior cells and do not involve changes in cell volume. Wireframe reconstructions of the tail tip cells before (A, C, E, G) and during retraction (B, D, F, H) (cf. Figs. 2 and 3). Scale bar, 10 μm. Anterior is to the upper left. Positions of the nuclei are noted (n). Cell boundaries were traced for several sections of hyp11 and hyp8 in a stage 0 male (A, C) and in an example of precocious retraction in a stage 1 male (B, D). Small arrows (in A and C) indicate portions of the cells initially near the body wall that retract toward the central core. Large arrowheads indicate the main direction of retraction. The anterior left arm of hyp11 becomes enlarged, but does not extend much further rostrally, while the semicircular cell border apposed to the dorsolateral cuticle in the posterior half is reduced. The soma of hyp8 becomes rostrally enlarged and extended, while its semicircular border with the ventrolateral cuticle is less extensive than at stage 0. Tracings from hyp10 and hyp9 in a stage 0 male (E, G) and a stage 3 male (F, H) demonstrate marked changes in shape but not volume during the retraction of these cells.

Staining *lep-1* mutants with the MH27 antibody shows that fusions of the tail tip cells are delayed with respect to other morphogenetic events (in all 38 L4 and adult males that were closely observed), suggesting that the primary defect in these mutants may be in a regulatory or triggering event common to both the fusion and retraction pathways. Whereas fusions of at least hyp11 and hyp8 have begun by the time ray cells cluster at stage 1 in wild-type males (Figs. 5C and 5D), tail tip cells in most *lep-1* specimens at this stage have not yet fused (Figs. 8A and 8B). In many cases (5/10 of the stage 2 males and 3/9 of the adult males closely observed), hyp10 fusion with the other tail tip cells is greatly delayed or fails altogether, as indicated by persistence of adherens junctions surrounding hyp10 at stage 2 (Figs. 8C and 8D) or even in the adult (Figs. 8E and 8F). That hyp10 fusions are invariably the most delayed in *lep-1* mutants is also consistent with a posteriorward progression of cell fusions in wild-type animals.

Leptoderan tail tips occur naturally in many species that are fairly closely related to *C. elegans* (Sudhaus, 1976). As in *lep-1* mutants of *C. elegans*, these leptoderan tail tips result when the tail tip cells fail to retract (e.g., as in *O. myriophila;* Figs. 1H–1L). In all leptoderan species observed so far, the tail tip cells either fail to fuse at all (as in *Rhabditella axei*, $N > 50$, Figs. 9D–9F; and *O. myriophila*, $N > 50$, not shown) or only hyp10 fails to fuse with the other tail tip cells (as in an undescribed *Rhabditis* species, $N > 10$, Figs. 9A–9C).

TABLE 2
Nuclear Migration during Tail Tip Development

Stage[b]	Sex	Series	Distance of hyp nucleus behind phasmid opening (μm)[a]				
			hyp10-1	hyp10-2	hyp9	hyp11	hyp8
0	M	19	15.3	11.2	8.8	2.8	1.8
1	M	17	19.2	14.1	11.4	4.8	3.9
1	M	16B	14.7	10.7	7.2	3.1	1.4
2	M	18A	17.4	13.5	8.2	3.1	1.3
2	M	16A	?[c]	11.7	7.8	3.3	3.9
2	M	18B	15.4	11.6	7.3	0.8	1.6
3	M	21	?[c]	1.5	1.0	−4.0	?[c]
3	M	20A	1.3	0.2	−3.0	−6.0	−6.3
L4	H	20B	16.6	11.9	7.0	6.5	2.5
Adult	H	B116	0.1	−0.9	−4.1	−5.4	−7.8

[a] Distance was measured by section number (0.06 μm per section) and therefore represents distance only along the anteroposterior axis. Negative distances indicate that nuclear positions are anterior of the phasmid opening.
[b] See text for staging of L4 males.
[c] These nuclei were not seen in available sections.

Summary of Results

Our data define the following highlights of male tail tip morphogenesis (schematized in Fig. 10).

1. All fusions of the tail tip hypodermal cells (hyp8–hyp11) occur at sites corresponding spatially to the adherens junctions. These data are consistent with a localization of fusogenic proteins to adherens junctions linking the tail tip cells.

2. However, not all hypodermal adherens junctions in *C. elegans* correspond to fusion sites. For example, the male-specific hyp13 compartment we discovered does not fuse when the adjacent tail tip cells fuse. This suggests that only particular cells are competent to fuse; e.g., fusogenic components are expressed or activated in a highly localized manner.

3. Although the tail tip cells in the different sexes have identical lineages and morphology until the last larval stage, their environments differ. For example, in males, hyp8 contacts the hyp13 compartment (which is fused with hyp7 and is not a separate compartment in hermaphrodites). In males, the tail tip cells also make contacts with cells associated with the male-specific ray lineages (e.g., R9.p). These sex-specific environments could differentially affect tail tip cell fate.

4. Tail tip cell fusions begin anteriorly and progress

TABLE 3
Relative Volumes of Tail Tip hyp Cells, Vacuoles, and Extracellular Spaces

Stage	Series	Sex	Relative volume (% of tail tip or hyp cell)[a]								
			hyp10	hyp10 vacuoles	hyp9	hyp9 vacuoles	hyp11	hyp11 vacuoles	hyp8	hyp8 vacuoles	*E*
L4	20B	H	27	5.1	27	14.5	21	18.3	24	12.7	6.8
0	19	M	20	2.9	23	4.6	29	2.3	28	2.2	5.3
1	16B	M	19	2.4	29	8.3	21	33.3	30	2.6	4.6
1	17	M	25	4.3	23	15.0	25	20.2	27	16.2	4.6
2	18B	M	20	2.7	20	14.5	32	13.7	29	39.5	3.4
2	18A	M	23	6.4	25	10.0	26	11.1	26	12.2	4.4
3[b]	20A	M	18	6.1	23	3.2	32	2.1	23	1.4	46.8

[a] Because absolute volumes were subject to large systematic error due to assumptions of section thickness, all cell volumes are normalized as a percentage of the combined volumes of all four tail tip hyp cells. Similarly, total volumes of the vacuoles for each cell are normalized as a percentage of that cell's cytoplasmic volume. Extracellular volumes (*E*) are normalized as a percentage of the total tail tip hyp cell volumes. The largest relative vacuolar volumes have been highlighted.
[b] To calculate cell volumes of fusing cells, the cell boundaries had to be extrapolated.

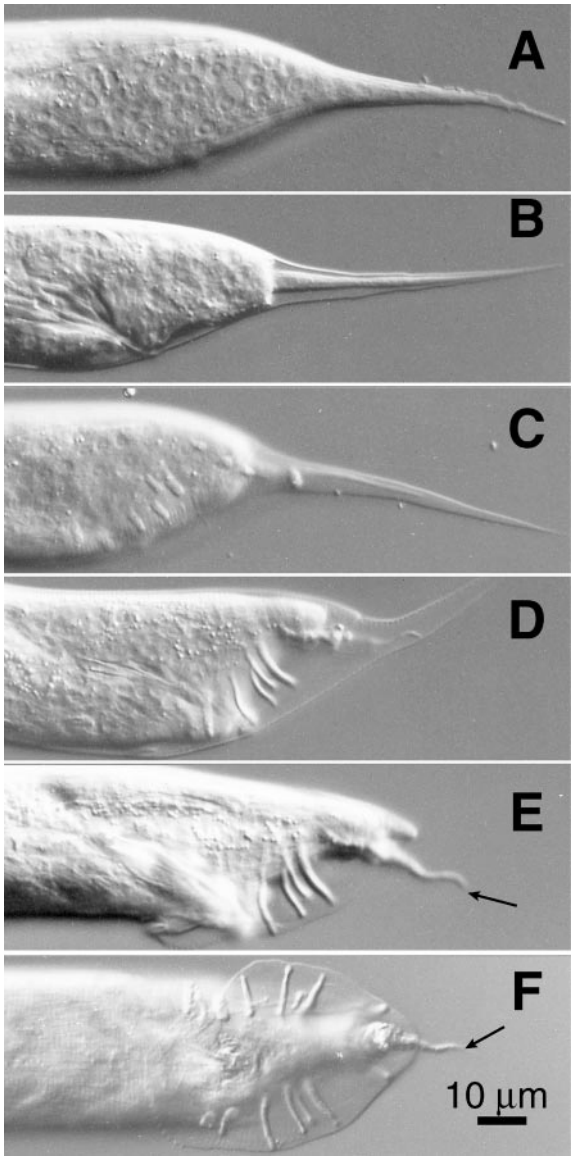

FIG. 7. In *lep-1(bx42)* mutants, tail tip retraction fails (A–D), forming a "leptoderan" adult tail (arrows in E and F; left lateral and ventral views), yet the male fan and rays are normal. Note that fluid still accumulates in the extracellular space while a leptoderan tail tip is maintained (B–D).

posteriorly. In *lep-1* mutants, this progression is more marked because of its delay (Fig. 8).

5. Changes in tail tip cell shape (Fig. 6) also begin with the anterior cells hyp11 and hyp8. Tail tip morphogenesis thus appears to be initiated anteriorly.

6. Changes in tail tip cell shape (Fig. 6) do not involve changes in relative cell volumes.

7. Although tail tip cell fusions and shape changes generally occur at the same developmental stage, shape changes may sometimes occur before fusions. Thus, fusions are probably not required for shape change. However, in *lep-1* mutants, both events are delayed, suggesting they are coordinately regulated at some level.

8. Although adherens and gap junctions link the tail tip hyp cells (Table 1), they do not link every cell to every other cell in parallel. If morphogenesis is coordinated by a signal associated with either type of junction, such a signal would in some cases have to be transduced via an intermediate cell in series.

9. Fluid is excreted into the extracellular space posterior of the tail tip cells, but the relative volumes of the tail tip cells do not change. However, volumes of vacuoles in the tail tip cells do appear to vary with developmental stage. Perhaps this vacuolar system has been recruited during male tail morphogenesis to move fluid into the extracellular space via the tail tip hyp cells.

DISCUSSION

To explore the mechanisms of morphogenesis, it is first necessary "to understand the interactions between the cells and the environment in which they operate" (Bard, 1992, p. 3). Consequently, a detailed delineation of the morphogenetic process, as we have attempted for the *C. elegans* tail tip, is required because "it is only by knowing *what* happens that we can pose questions about *how* it happens" (Bard, 1992, p. 24). Serial thin sections and immunofluorescent staining of adherens junctions not only delineate the major cellular events underlying male tail tip morphogenesis but also suggest sites of action and possible mechanisms.

First, there appear to be two independent morphogenetic mechanisms in the male tail, one that involves retraction of only the tail tip cells and another that involves the other portions of the male tail (including the ray cells and cells of the B lineage located more internally). In *lep-1* mutants and leptoderan nematode species, retraction of the tail tip fails, but general male tail retractions still proceed to form the fan and rays. Indeed, *lep-1* males have wild-type mating efficiency and behavior (Y.Y. and D.H.A.F., unpublished), consistent with restriction of the effects of reduced-function *lep-1* mutations to the tail tip. We have focused specifically on the tail tip mechanism.

Second, there are four main events that occur during male tail tip morphogenesis (Fig. 10). (1) Morphogenesis is triggered probably by a signal originating anterior to the tail tip cells (large green arrow in Fig. 10A). (2) The tail tip hyp cells fuse to each other at the adherens junctions (dashed red lines in Figs. 10A and 10B); these fusions are initiated anteriorly and progress posteriorly. (3) Fluid appears to be transferred by transcytosis (gold arrows in Fig. 10B) through the tail tip cells by vacuoles (gold spheres in Fig. 10B) to extracellular spaces and eventually accumulates in the tail spike (gold area in Fig. 10C). (4) The cells (or syncytium) change shape and retract (violet arrows in Fig. 10C), the

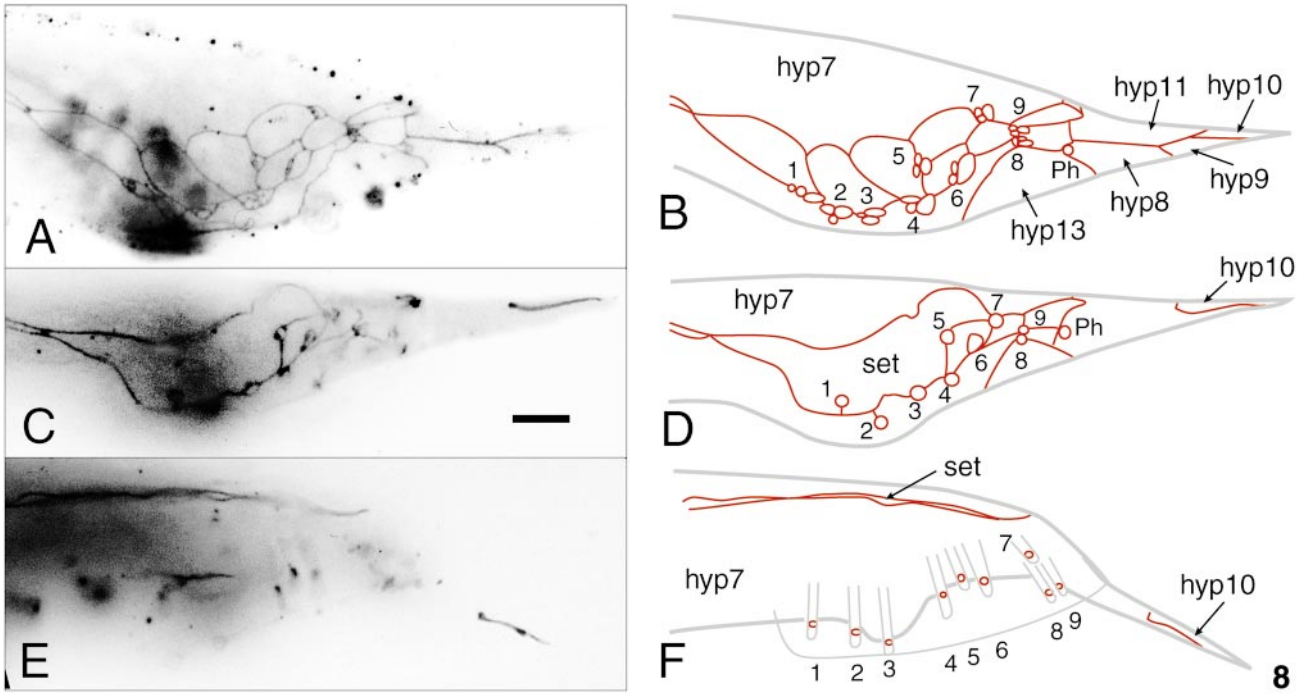

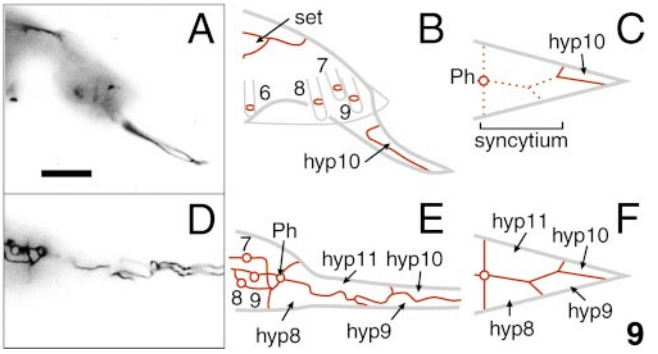

FIG. 8. Early stages in *lep-1(bx42)* male tail development viewed by MH27 staining. The layout is similar to that in Fig. 4, except that the stages depicted in A & B and C & D correspond to stages shown in C & D and E & F of Fig. 4. Scale bar, 10 μm. E and F show an adult male with the mature positions of the "set" and the nine sensory rays with respect to the cuticular fan. Note the presence of a nonretracted, leptoderan tail tip posterior of the fan. During tail tip cell fusions in *lep-1* mutants, the hyp10 cell fails to fuse with its anterior neighbors, as inferred from persistence of MH27 staining at its border.

FIG. 9. Leptoderan male tail tips of an adult *Rhabditis* sp. (A–C) and a stage 3 *Rhabditella axei* (D–F) compared using MH27 staining (A, D), tracings of the staining (red lines, B and E), and schematic models (C, F). In *Rhabditis* sp., only hyp10 remains unfused, much like the *lep-1* mutation of *C. elegans*. In *Rhabditella axei*, all the tail tip cells remain unfused and none retract.

syncytium moves anteriorward (orange arrow in Fig. 10C), and the nuclei (blue ovals in Figs. 10A–10C) are translocated anteriorly past the phasmid openings (Ph, Figs. 10A–10C). These events are coordinated (e.g., through a genetic pathway that may include *lep-1*) during the mid-L4 stage just after male-specific cell proliferations have been completed.

Tail Tip Retraction Results from a Change in Cell Shape and Possibly Cell "Crawling"

Several lines of evidence suggest that cell fusion and fluid transfer may not be required for the changes in tail tip cell shape that accompany the first step of retraction (Fig. 1A to Fig. 1B). (1) Even though hyp8, hyp9, hyp11, and sometimes

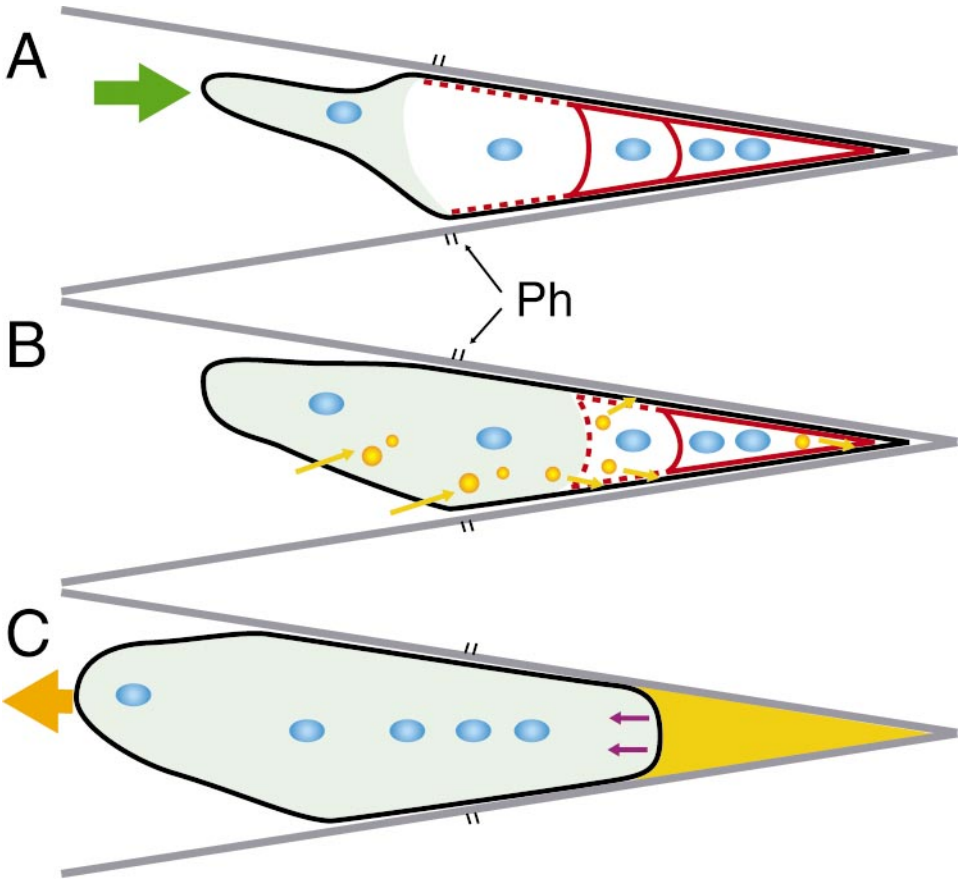

FIG. 10. A model for L4 male tail tip morphogenesis in *C. elegans*. A ventral view is schematized. Anterior is left, left is up. Ventral and lateral adherens junctions between the tail tip hyp cells (hyp8–hyp11) are shown as red lines. For simplicity, junctions between other cells (e.g., between hyp13 and hyp8 or between hyp11 and other male-specific cells) are not shown. The lateral outline of the tail tip hypodermis is shown as a black line and the L4 cuticle as a thicker gray line. The phasmid openings in the cuticle are indicated as short black parallel lines (Ph). Nuclei are represented as blue ovals. In A, the anterior portion of hyp11 is shown in light green shading, but from this ventral perspective the rest of hyp11 lies behind (dorsal to) hyp8. The only adherens borders between hyp11 and hyp8 are lateral, not ventral. (A) At stage 1, probably in response to a trigger from a source anterior to the tail tip hyp cells (large green arrow), the anterior tail tip hyp cells begin to fuse (dashed red lines). These fusions are initiated at the adherens junctions and progress posteriorly. (B) Fluid from cells lying anterior to the tail tip may be taken up (gold arrows) into vacuoles (gold spheres). At stage 2, the cell fusions are nearly complete (the syncytium is represented by the light green area); hyp10 is the last cell to fuse. The anterior cells (hyp8 and hyp11) begin to show signs of cell shape change. Meanwhile, vacuoles may transport fluid posteriorly by transcytosis. (C) At stage 3, the tail tip cells have completely fused to form the tail tip syncytium (light green area). Fluid is dumped, presumably by the vacuoles (gold spheres) into the extracellular space (gold area) that forms at the posterior end between the L4 cuticle and the tail tip hypodermis. The posterior end of the tail tip hypodermis retracts anteriorly at first because of a change in hyp9 and hyp10 cell shape (violet arrows; see also Fig. 6). The tail tip hypodermis continues retracting anteriorly (orange arrow), perhaps by a cell-crawling mechanism. Both the fusions and the retraction are coordinately controlled (e.g., through a genetic pathway that includes *lep-1*). Several aspects of this model remain hypothetical; in particular, the mechanism of fluid expulsion, the nature of the trigger, the mechanism of retraction, and the genetic pathway(s) that govern tail tip morphogenesis.

hyp10 are fused in *lep-1* males (albeit fusions are delayed), tail tip retraction fails, suggesting that fusions are not sufficient for retraction. (2) Although hypertonic solutions appear to reduce general male tail retraction, tail tip retraction is not affected by hypertonic conditions (S. Emmons, personal communication; D.H.A.F., unpublished; discussed later), suggesting that fluid expulsion is required for general male tail retraction but not tail tip retraction. (3) In *lep-1* mutants and leptoderan species, fluid expulsion still occurs to allow general male tail retraction but the tail tip fails to retract (Fig. 1), suggesting that fluid expulsion is not sufficient for tail tip retraction. (4) In one L4 male examined by EM, retraction of the tail tip had begun before fluid expulsion, causing the distal portion of the tail spike to shorten

and warp. One possible mechanism for the observed changes in cell shapes (as well as the nuclear migrations) is an active change in the architecture of the cytoskeleton in these cells, although any such change in the organization of cytoskeletal actin microfilaments was not observable in our EM studies.

We speculate that the observed changes in cell shape (as well as the nuclear migrations) may also result from the participation of at least hyp11 and hyp8 in a crawling phase, similar to the known migrations of some neurons, muscle precursors, muscle arms, and other mesodermal processes (Hedgecock *et al.,* 1987). In particular, the shape of the migrating hypodermal tissue is remarkably similar to the shape of the distal tip cell (DTC) of the gonad (D.H.H. and E. Hedgecock, unpublished). As with the DTC, the hypodermal migration involves a broad, blunt leading edge of tissue juxtaposed closely to the basal lamina, with the cell nucleus pressed close to the lead and with thinner processes trailing behind the cells. An extrinsic signal expressed in the basal lamina could guide or stimulate this migration, much as netrin is known to guide the motion of many classes of cells in earlier stages of development (Wadsworth *et al.,* 1996). Although no changes in the actin cytoskeleton (as might be expected in a crawling cell) were observable in our study, morphogenesis fails in treatments with cytoskeletal inhibitors (K. L. Chow and Y. Tse, personal communication). Alternatively, continued anterior migration of the tail tip cells is also compatible with these cells being passively drawn forward by their connections with anterior cells undergoing active morphogenetic movements.

Tail Tip Cell Fusions Probably Initiate at Adherens Junctions

Particular membrane proteins are generally required to hold cells in close proximity before fusogenic proteins can act. In some mutants that block fusion in *Drosophila,* dense membrane plaques between unfused myoblasts (*rolling stone*) or membrane-bound vesicles lining the cell border (*blown fuse*) accumulate to abnormally high levels; in other mutants, all such membrane-associated structures are absent (*myoblast city*) (Rushton *et al.,* 1995; Doberstein *et al.,* 1997; Paululat *et al.,* 1995). These symmetrical junctional structures are postulated to be part of the prefusion complex in fly myoblasts, perhaps delivering or holding fusogenic moieties in place on both membranes prior to fusion. Similarly, gap junctions have been reported to be a necessary precursor to a fusion event in some vertebrate myoblasts, and specific channel blockers can inhibit cell fusions (Proulx *et al.,* 1997). Adherens junctions are required at some sites of cell fusion, apparently to help localize signaling or fusogenic molecules (Doberstein *et al.,* 1997).

We speculate that adherens junctions provide such a function in the tail tip cells. Unlike *Drosophila* myoblast fusions, no obvious prefusion complexes or vesicles participate in initiating tail tip cell fusions. Perhaps other adjoining cells (hyp13, hyp7) are protected from fusion into the same compartment during tail tip morphogenesis either by failure to express, activate, or localize the fusogenic moiety or by expressing an inhibitory molecule.

While this paper was being reviewed, Mohler *et al.* (1998) showed that hypodermal fusions during *C. elegans* embryogenesis also originate at or near adherens junctions. That is, in both the tail tip and the embryonic fusions, the fusing membranes are first held closely together by an adherens plaque, with fusion pore formation occurring at or very near the plaque. However, two details of the tail tip and embryonic mechanisms look slightly different. (1) During the embryonic fusions, the adherens junctions do not immediately disappear, but retreat away from the body wall toward more basal portions of the cell border, leading a front of fusions between adjacent cells beginning apically and progressing basally. Using multiphoton imaging, Mohler *et al.* (1998) detected internalization of the MH27 epitope (adherens junction material) into more basal portions of the cell border. They also suggested a mechanism where the first step is the formation of a small fusion pore at the apical border, followed by rapid radial destruction of the cell border. In the tail tip, we did not observe any basally translocated MH27 epitope or adherens plaque by immunofluorescence or EM. The resolution of our epifluorescence may not have allowed us to visualize this basal migration of epitope; also, a low concentration of MH27 epitope in the retreating membrane may not have been morphologically distinguishable by EM. (2) By EM, Mohler *et al.* detected a fine vesiculation of the internalized, dispersing membranes before they were fully digested. These fine vesicles may correspond to the membrane fragments and larger membranous circles that we detect at former cell borders; minor variations in EM fixation methods could also be responsible for such differences. There is no evidence from either study that "prefusion complexes" such as those required for *Drosophila* myoblast fusions (Doberstein *et al.,* 1997) participate in these *C. elegans* fusions.

What fusogenic molecules might be involved? In other systems, the lipid bilayer surrounding a fusing virus, vesicle, or cell carries a membrane-spanning protein which is complementary to another membrane-spanning protein carried on the surface of the fusion partner; e.g., viral fusion proteins (hemagglutanins), v-SNAREs and T-SNARES for vesicle release, or ADAMs for cell fusion (White, 1992; Kemble *et al.,* 1994; Lindau and Almers, 1995; Huovila *et al.,* 1996; Myles and Primakoff, 1997; Weber *et al.,* 1998). In *C. elegans,* ADM-1, an ADAM protein with sequence similarity to metalloprotease-like fusogenic proteins, is expressed in hypodermis at times of cell fusion (Podbilewicz, 1996). However, no male tail phenotypes have been described. Male phenotypes are observed in mutants of *sup-17,* which encodes another ADAM protein known to interact with the LIN-12/NOTCH receptor (Wen *et al.,* 1997), but not known to be involved in cell fusions.

How Is Tail Tip Morphogenesis Triggered?

The competence of tail tip cells to undergo male-specific tail tip morphogenesis could be determined either autonomously or nonautonomously. For example, male-specific fate of the tail tip cells could be determined by the somatic sex-determination pathway in which the gene *tra-1* is required and sufficient for cell-autonomous specification of hermaphrodite fate (except in the vulval precursor cells, which are nonautonomously specified) (Hunter and Wood, 1990). However, *lep-1 tra-1* double mutants still make leptoderan tail tips, suggesting that *tra-1* function is not required to make pointy tail tips (Y.Y. and D.H.A.F., unpublished). Also, mosaics have not yet been reported in which *tra-1(+)* tail tip hyp cells in an otherwise *tra-1(−)* male tail fail to retract. It is possible that the tail tip cells in both hermaphrodites and males are competent to undergo morphogenesis, but that external male-specific cues (such as a hypothetical signal from adjacent male-specific cells) determine the adult male-specific fate of the tail tip hyp cells.

Once competence is determined, male tail tip morphogenesis itself could be triggered either autonomously by some internal mechanism or nonautonomously by signaling from the environment around the tail tip cells. We favor the latter hypothesis because of the following. (1) The tail tip cells arise very early from embryonic lineages, yet their morphogenesis only occurs very late during postembryonic development. (2) Tail tip retractions often fail in mutants with normal tail tip lineages but disrupted ray cell lineages (discussed later). Whatever triggers morphogenesis, our data are also consistent with a trigger originating at the anterior of the tail tip compartment: tail tip hyp cell fusions progress from anterior to posterior (Fig. 4) and changes in tail tip cell shape begin anteriorly (Fig. 6). Interestingly, an anterior–posterior directionality of cell fusions in hypodermis has been reported in several other regions during both embryonic and postembryonic development of the hermaphrodite (Podbilewicz and White, 1994).

Where might an external trigger signal originate? One hypothetical candidate is a hormonal signal (such as might be involved in the heterochronic pathway, discussed later; Slack and Ruvkun, 1997). Presumably, a hormonal signal could originate anteriorly and move posteriorly down the body. That other postembryonic fusions in the hermaphrodite and the male have the same polarity (Podbilewicz and White, 1994; Fitch and Emmons, 1995) is consistent with such a notion. The microanatomical work we have presented also allows the identification of other candidate sources for a hypothetical triggering signal. For example, male-specific cells lie adjacent to and share adherens junctions with the tail tip cells, namely the bilateral pairs of R9.p and R8.p cells. A priori, the male-specific hyp13 syncytium might not seem to be a good candidate because it is also present very early during larval male development when tail tip morphogenesis does not occur. However, hyp13 itself could be triggered by other male-specific cells to transduce a signal secondarily to the tail tip cells. The distinctive, forward-reaching arm of hyp11 suggests that this cell has the best opportunity to receive signals from several different anterior cells.

If morphogenesis is triggered nonautonomously, we might expect hypomorphic mutations in particular signaling pathways to disrupt morphogenesis and result in leptoderan tail tips. Although our genetic survey has not been exhaustive, we have not yet identified a good candidate cell–cell signaling pathway that triggers male tail tip morphogenesis. For example, cadherins may be coupled to signal transduction pathways or might themselves transduce signals (Gumbiner, 1996). Although the CDH-3 cadherin is required for proper embryonic morphogenesis of hyp10, a presumptive null mutation does not affect male tail morphogenesis (Pettitt *et al.*, 1996). *lin-44* hypomorphs are the only signal pathway mutants we have observed so far to produce leptoderan tail tips, albeit at low penetrance (about 10%). We interpret this phenotype, however, not as a direct effect of reduced LIN-44 induction of tail tip morphogenesis, but as a secondary effect of the variably disrupted lineages from the T blast cell (see Herman and Horvitz, 1994). That is, the posterior three rays (7–9), R7.p–R9.p cells, and phasmid cells are derived from the T cell. If a non-LIN-44 signal inducing tail tip morphogenesis were normally produced by any of these cells, inverting the division asymmetries of their progenitors by reducing LIN-44 function might interpose nonsignaling cells between the tail tip and the signaling cell(s). The low (ca. 10%) penetrance of the leptoderan phenotype might result from redundancy of the signal, variability in the lineage defects, or variable effects on the fates of cells producing the putative signal. Other mutations in genes not directly involved in signaling pathways are consistent with this interpretation. For example, leptoderan tail tips occur at low penetrance (ca. 10%) in *mab-19* mutants which variably affect the T lineages in males (Sutherlin and Emmons, 1994). Another mutation, *sy68*, produces leptoderan tail tips but also affects the ray lineages (H. Chamberlin and P. Sternberg, personal communication; our observations).

Tail Tip Morphogenesis Is Delayed in lep-1 Mutants

The phenotype of the *lep-1* mutants is informative in several ways about the morphogenetic mechanism. First, because the fan and rays are always normal in these mutants, not all of the components required for tail tip retraction are necessary for fan and ray morphogenesis. Second, both tail tip cell fusions and retraction appear to be affected, suggesting that these two processes are not only contemporaneous, but may also be regulated coordinately at some point in the pathway. Third, the delayed fusions are most pronounced for the most posterior cell, consistent with a signaling wave that might originate anteriorly and progress posteriorly. Finally, these mutations point to a component, encoded by the *lep-1* locus, that regulates or participates in the morphogenetic mechanism. We are currently isolating this gene and have

initiated screens for more leptoderan mutants to identify additional components.

Additional Regulatory Pathways Govern Tail Tip Morphogenesis

Other mutations point to the possible involvement of the sex-determination and heterochronic regulatory pathways. For example, leptoderan tail tips are produced infrequently by mutations at the *mab-3* locus, which may be required for responding to the sex-determination pathway (Shen and Hodgkin, 1988). The leptoderan phenotype has been interpreted as a sexual transformation to the hermaphrodite fate (Shen and Hodgkin, 1988; Hodgkin, 1997, p. 979). Alternatively, the appearance of leptoderan tail tips could be correlated with morphological defects in cells derived from T and adjacent to the tail tip (Shen and Hodgkin, 1988). That is, the possibility remains that the tail tip cells are not intrinsically sex transformed in *mab-3* mutants, but that a putative signal either triggering or determining retraction is sometimes missing due to variable defects in the lineages or differentiation of cells that would normally produce this signal. Perhaps sexual dimorphism in this structure primarily results from cues extrinsic to the tail tip itself.

Leptoderan tails also result (at high penetrance) from mutations in some genes (e.g., *let-7*) of the heterochronic pathway (M. Basson, H. R. Horvitz, and F. Slack, personal communication), which regulates the stage specificity of developmental events (reviewed by Ambros, 1997; Slack and Ruvkun, 1997). The leptoderan phenotype in these cases could be interpreted as resulting from a heterochronic delay in the adult program. Perhaps the trigger and/or the competence of the tail tip cells for morphogenesis requires the "larval-to-adult" switch governed by the heterochronic pathway.

The Tail Tip May Transport Fluid during Male Tail Morphogenesis

The large intracellular vacuoles that appear and disappear during male tail morphogenesis may underlie a mechanism for the translocation of fluid from anterior regions into extracellular spaces during morphogenesis. During morphogenesis, the cytoplasmic volumes of the tail tip cells themselves remain surprisingly constant instead of decreasing in proportion to the increase in extracellular volume (although their shapes change; see Fig. 6). This suggests that the intracellular vacuoles swell by uptake of fluid not from the tail tip cells themselves, but from another source, presumably anterior to the tail tip cells. One hypothesis is that fluid originating anteriorly from the pseudocoelom is transported into the tail tip cells by transcytosis. In this model, the tail tip cells act as the most posterior members in a chain of transporters. If so, one might also expect mutations in genes affecting endo- or exocytosis to affect general male morphogenesis. Indeed, male tail defects are associated with reduced-function mutations of *unc-101*, a gene encoding a clathrin adaptor (Lee *et al.*, 1994). Interestingly, the large intracellular vacuoles are not themselves sex specific; hermaphrodite larvae and adults have them as well (Table 3). We speculate that during the evolution of male tail morphogenesis, this vacuolar system may have been recruited as a mechanism to remove fluid from the tail to allow retraction in the formation of the fan and rays.

One role for exocytosis might be to provide a hydrostatic mechanism to push the tail tip cells forward during retraction. When a laser microbeam is used to puncture the L4 cuticle just at the time of tail tip retraction, or L4 worms are immersed in hypertonic solution, severe defects in adult male tail morphology can result (S. Emmons, personal communication; D.H.A.F., unpublished). However, pointy leptoderan tail tips are not formed, arguing against a major role of exocytosis in driving tail tip morphogenesis per se. The entire worm body is maintained under hydrostatic pressure that is controlled by an osmoregulatory system (Wood, 1988). The gross male tail defects could be produced simply by releasing this pressure posteriorly as opposed to eliminating a hydrostatic mechanism specifically driving anterior migration. Also, leptoderan tail tips in *C. elegans* mutants or other species are formed even as fluid accumulates in the extracellular space. Thus, removal of fluid from the male tail by exocytosis and the change in tail tip cell shape may be independent processes. On the other hand, the possibility that cytoskeletal components are involved in male tail morphogenesis (e.g., as might be predicted if the hypodermal cells crawl forward) is supported by the morphogenetic failures that result from treatments with cytoskeletal inhibitors (K. L. Chow and Y. Tse, personal communication).

Syncytial Compartments Help Organize the Body Plan and Allow Mosaic Evolution

Epidermal compartmentalization created by cell fusion may allow a certain degree of mosaic evolution, whereby different compartments evolve somewhat independently. Fusion permits cells within a compartment to be regulated coordinately. In the case of the male tail, the four tail tip hyp cells constitute a posterior compartment of hypodermis—independent of the hypodermal compartments in which the fan and rays form—which can be remodeled to form the blunt tip of the male bursa. For example, some mutations produce leptoderan tails without disrupting morphogenesis of the fan and rays. Similar variations have been fixed during evolution. In Rhabditidae, fan and tail tip compartments have evolved fairly independently (Sudhaus and Fitch, in press). Changes in these features have arisen independently in different lineages, producing morphologically diverse broad-fanned peloderan species (e.g., in *Caenorhabditis*), leptoderan species with well-developed fans (e.g., in *Oscheius*), or leptoderan species with rudimentary fans (e.g., in *Rhabditella*) (Sudhaus, 1976). However, we have not yet found peloderan species with rudimentary fans in Rhabditidae. This may result

more from selection than from developmental nonindependence between fans and tail tips. For example, fans may be required as "suction cups" for stabilizing mating in cases where long leptoderan tail tips are absent; long leptoderan tail tips appear to stabilize mating in a different way—by coiling around the female.

The male tail tip also provides an excellent opportunity to discover how morphological diversity results from evolutionary changes. In the leptoderan species *R. axei* and *O. myriophila,* tail tip cells fail to fuse and retract; in a *Rhabditis* species, the anterior tail tip cells fuse, but the hyp10 homolog fails to fuse and retraction fails. The latter example looks strikingly similar in these minute cellular details to the *lep-1* mutants of *C. elegans.* Differences between peloderan and leptoderan species might be due to change(s) at some step in the genetic pathway in which *lep-1* is involved, at the *lep-1* locus itself, or in a parallel pathway (see Fitch, 1997).

Our reconstruction of male tail tip morphogenesis shows that several cellular processes such as fusion, change in cell shape, and fluid displacement are coordinated and precisely timed to occur at the mid-L4 stage. These data provide a backdrop for future studies to uncover the complete developmental programs and genetic regulatory networks that produce this simple multicellular structure, determine its sexual dimorphism, and change through evolution.

ACKNOWLEDGMENTS

We are indebted to M. Basson, H. Chamberlin, K. L. Chow, S. Emmons, H. R. Horvitz, B. Podbilewicz, F. Slack, and Y. Tse for communication of results before publication. We gratefully acknowledge S. Emmons, G. Kao, A. Rougvie, P. Sternberg, and W. Wadsworth for sending strains; R. Barstead and R. Waterston for MH27 antibody; and L. Hall for help in illustrations. We thank S. Emmons, J. Hubbard, and S. Small for enlightening discussions and two anonymous reviewers for their insightful and constructive comments on the manuscript. The *Caenorhabditis* Genetics Center, which is supported by the NIH Center for Research Resources, provided some of the strains. This work was funded by NSF Grant IBN-9506844 and an NYU Whitehead Fellowship to D.H.A.F. and NIH Grant RR12596 (NCRR) to D.H.H. for the Center for *C. elegans* Anatomy.

REFERENCES

Ambros, V. (1997). Heterochronic genes. *In* "*C. elegans* II" (D. L. Riddle, T. Blumenthal, B. J. Meyer, and J. R. Priess, Eds.), Chap. 18, pp. 501–518. Cold Spring Harbor Laboratory Press, Cold Spring Harbor, NY.

Andrássy, I. (1983). A taxonomic review of the suborder Rhabditina (Nematoda: Secernentia). Office de la Recherche Scientifique et Technique Outre-Mer, Paris.

Baird, S. E., Fitch, D. H. A., Kassem, I., and Emmons, S. W. (1991). Pattern formation in the nematode epidermis: Determination of the spatial arrangement of peripheral sense organs in the *C. elegans* male tail. *Development* **113,** 515–526.

Bard, J. (1992). "Morphogenesis: The Cellular and Molecular Processes of Developmental Anatomy." Cambridge Univ. Press, Cambridge.

Bossinger, O., and Schierenberg, E. (1992). Cell–cell communication in the embryo of *Caenorhabditis elegans. Dev. Biol.* **151,** 401–409.

Brenner, S. (1974). The genetics of *Caenorhabditis elegans. Genetics* **77,** 71–94.

Chitwood, B. G., and Chitwood, M. B. (1950, 1974). "Introduction to Nematology." Univ. Park Press, Baltimore.

Doberstein, S. K., Fetter, R. D., Mehta, A. Y., and Goodman, C. S. (1997). Genetic analysis of myoblast fusion: *blown fuse* is required for progression beyond the prefusion complex. *J. Cell Biol.* **136,** 1249–1261.

Emmons, S. W., and Sternberg, P. W. (1997). Male development and mating behavior. *In* "*C. elegans* II" (D. L. Riddle, T. Blumenthal, B. J. Meyer, and J. R. Priess, Eds.), Chap. 12, pp. 295–334. Cold Spring Harbor Laboratory Press, Cold Spring Harbor, NY.

Finney, M., and Ruvkun, G. (1990). The *unc-86* gene product couples cell lineage and cell identity in *C. elegans. Cell* **63,** 895–905.

Fitch, D. H. A. (1997). Evolution of male tail development in rhabditid nematodes related to *Caenorhabditits elegans. Syst. Biol.* **46,** 145–179.

Fitch, D. H. A., and Emmons, S. W. (1995). Variable cell positions and cell contacts underlie morphological evolution of the rays in the male tails of nematodes related to *Caenorhabditis. Dev. Biol.* **170,** 564–582.

Fitch, D. H. A., Bugaj-Gaweda, B., and Emmons, S. W. (1995). 18S ribosomal RNA gene phylogeny for some Rhabditidae related to *Caenorhabditis. Mol. Biol. Evol.* **12,** 346–358.

Francis, G. R., and Waterston, R. H. (1985). Muscle organization in *C. elegans:* Localization of proteins implicated in thin filament attachment and I-band organization. *J. Cell Biol.* **101,** 1532–1549.

Geiger, B., Yehuda-Levenberg, S., and Bershadsky, A. D. (1995). Molecular interactions in the submembrane plaque of cell–cell and cell–matrix adhesions. *Acta Anat.* **154,** 46–62.

Gumbiner, B. M. (1996). Cell adhesion: The molecular basis of tissue architecture and morphogenesis. *Cell* **84,** 345–357.

Hall, D. H. (1977). The posterior nervous system of the nematode *Caenorhabditis elegans.* Ph.D. Thesis. California Institute of Technology, Pasadena.

Hall, D. H. (1987). Freeze fracture and freeze etch studies of the nematode, *Caenorhabditis elegans. N.Y. Acad. Sci.* **494,** 215–217.

Hall, D. H. (1995). Electron microscopy and three-dimensional image reconstruction. *In* "Methods in Cell Biology (L. Wilson and P. Matsudaira, Ser. Eds.), Vol. 48, *Caenorhabditis elegans:* Modern Biological Analysis of an Organism" (H. R. Epstein and D. C. Shakes, Eds.), Chap. 17, pp. 395–436. Academic Press, San Diego.

Hall, D. H. (1996). MH27 binds to several types of epithelial junctions by EM-immunocytochemistry in the nematode *C. elegans. Microsc. Microanal.* 26–27.

Hall, D. H., and Russell, R. L. (1991). The posterior nervous system of the nematode *Caenorhabditis elegans:* Serial reconstruction of identified neurons and complete pattern of synaptic interactions. *J. Neurosci.* **11,** 1–22.

Hedgecock, E., Culotti, J., Hall, D., and Stern, B. (1987). Genetics of cell and axon migration in *Caenorhabditis elegans. Development* **100,** 365–382.

Herman, M. A., and Horvitz, H. R. (1994). The *Caenorhabditis elegans* gene *lin-44* controls the polarity of asymmetric cell divisions. *Development* **120,** 1035–1047.

Hodgkin, J. (1988). Sexual dimorphism and sex determination. *In* "The Nematode *Caenorhabditis elegans*" (W. B. Wood, Ed.), pp. 243–279. Cold Spring Harbor Laboratory Press, Cold Spring Harbor, NY.

Hodgkin, J. (1997). Genetics. *In* "*C. elegans* II" (D. Riddle, T. Blumenthal, B. J. Meyer, and J. R. Priess, Eds.), Appendix 1, pp. 881–1047. Cold Spring Harbor Laboratory Press, Cold Spring Harbor, NY.

Hodgkin, J., Horvitz, H. R., and Brenner, S. (1979). Nondisjunction mutants of the nematode *Caneorhabditis elegans*. *Genetics* **91,** 67–94.

Hunter, C. P., and Wood, W. B. (1990). The *tra-1* gene determines sexual phenotype cell-autonomously in *C. elegans*. *Cell* **63,** 1193–1204.

Huovila, A-P. J., Almeida, E. A. C., and White, J. M. (1996). ADAMs and cell fusion. *Curr. Opin. Cell Biol.* **8,** 692–699.

Kam, Z., Minden, J. S., Agard, D. A., Sedat, J. W., and Leptin, A. (1991). *Drosophila* gastrulation: Analysis of cell shape changes in living embryos by three-dimensional fluorescence microscopy. *Development* **112,** 365–370.

Kemble, G. W., Danieli, T., and White, J. M. (1994). Lipid-anchored influenza hemagglutinin promotes hemifusion, not complete fusion. *Cell* **76,** 383–391.

Lee, J., Jongeward, G., and Sternberg, P. W. (1994). *unc-101*, a gene required for many aspects of *C. elegans* development and behavior, encodes a clathrin-associated protein. *Genes Dev.* **8,** 60–73.

Lindau, M., and Almers, W. (1995). Structure and function of fusion pores in exocytosis and ectoplasmic membrane fusion. *Curr. Opin. Cell Biol.* **7,** 509–517.

Mohler, W. A., Simske, J. S., Williams-Masson, E. M., Hardin, J. D., and White, J. G. (1998). Dynamics and ultrastructure of developmental cell fusions in the *Caenorhabditis elegans* hypodermis. *Curr. Biol.* **8,** 1087–1090.

Myles, D. G., and Primakoff, P. (1997). Why did the sperm cross the cumulus? To get to the oocyte. Functions of the sperm surface proteins PH-20 and fertilin in arriving at, and fusing with, the egg. *Biol. Reprod.* **56,** 320–327.

Newman, A. P., White, J. G., and Sternberg, P. W. (1996). Morphogenesis of the *C. elegans* uterus. *Development* **122,** 3617–3626.

Paululat, A., Burchard, S., and Renkawitz-Pohl, R. (1995). Fusion from myoblasts to myotubes is dependent on the *rolling stone* gene (*rost*) of *Drosophila*. *Development* **121,** 2611–2620.

Pettitt, J., Woold, W. B., and Plasterk, R. H. A. (1996). *cdh-3*, a gene encoding a member of the cadherin superfamily, functions in epithelial cell morphogenesis in *Caenorhabditis elegans*. *Development* **122,** 4149–4157.

Podbilewicz, B. (1996). ADM-1, a protein with metalloprotease- and disintegrin-like domains, is expressed in syncytial organs, sperm, and sheath cells of sensory organs in *Caenorhabditis elegans*. *Mol. Biol. Cell* **7,** 1877–1893.

Podbilewicz, B., and White, J. G. (1994). Cell fusions in the developing epithelia of *C. elegans*. *Dev. Biol.* **161,** 408–424.

Priess, J. R., and Hirsh, D. I. (1986). *Caenorhabditis elegans* morphogenesis: The role of cytoskeleton in elongation of the embryo. *Dev. Biol.* **117,** 156–173.

Proulx, A., Merrifield, P. A., and Naus, C. C. (1997). Blocking gap junctional intercellular communication in myoblasts inhibits myogenin and MRF4 expression. *Dev. Genet.* **20,** 133–144.

Rushton, E., Drysdale, R., Abmayr, S. M., Michaelson, A. M., and Bate, M. (1995). Mutations in a novel gene, *myoblast city*, provide evidence in support of the founder cell hypothesis for *Drosophila* muscle development. *Development* **121,** 1979–1988.

Shen, M. M., and Hodgkin, J. (1988). *mab-3*, a gene required for sex-specific yolk protein expression and a male-specific lineage in *C. elegans*. *Cell* **54,** 1019–1031.

Slack, F., and Ruvkun, G. (1997). Temporal pattern formation by heterochronic genes. *Annu. Rev. Genet.* **31,** 611–634.

Starich, T. A., Lee, R. Y. N., Panzarella, C., Avery, L., and Shaw, J. (1996). eat-5 and unc-7 represent a multigene family in *Caenorhabditis elegans* involved in cell–cell coupling. *J. Cell Biol.* **134,** 537–548.

Sudhaus, W. (1976). Vergleichende Untersuchungen zur Phylogenie, Systematik, Ökologie, Biologie und Ethologie der Rhabditidae (Nematoda). *Zoologica* **43,** 1–229.

Sudhaus, W., and Fitch, D. (in press). Comparative studies on the phylogeny and systematics of the Rhabditidae (Nematoda). Society of Nematologists, Lawrence, KS.

Sulston, J., and Hodgkin, J. (1988). Methods. *In* "The Nematode *Caenorhabditis elegans*" (W. B. Wood, Ed.), pp. 587–606. Cold Spring Harbor Laboratory Press, Cold Spring Harbor, NY.

Sulston, J. E., and Horvitz, H. R. (1977). Postembryonic cell lineage of the nematode *Caenorhabditis elegans*. *Dev. Biol.* **56,** 110–156.

Sulston, J. E., Albertson, D. J., and Thomson, J. N. (1980). The *Caenorhabditis elegans* male: Postembryonic development of nongonadal structures. *Dev. Biol.* **78,** 542–576.

Sulston, J. E., Schierenberg, E., White, J. G., and Thomson, J. N. (1983). The embryonic cell lineage of the nematode *Caenorhabditis elegans*. *Dev. Biol.* **100,** 64–119.

Sutherlin, M. E., and Emmons, S. W. (1994). Selective lineage specification by *mab-19* during *Caenorhabditis elegans* male peripheral sense organ development. *Genetics* **138,** 675–688.

Tanaka-Matakatsu, M., Uemura, T., Oda, H., Takeichi, M., and Hayashi, S. (1996). Cadherin-mediated cell adhesion and cell motility in *Drosophila* trachea regulated by the transcription factor Escargot. *Development* **122,** 3697–3705.

Wadsworth, W. G., Bhatt, H., and Hedgecock, E. (1996). Neuroglia and pioneer neurons express UNC-6 to provide global and local netrin cues for guiding migrations in *C. elegans*. *Neuron* **16,** 35–46.

Weber, T., Zemelman, B. V., McNew, J. A., Westermann, B., Gmachl, M., Parlati, F., Sollner, T. H., and Rothman, J. E. (1998). SNAREpins: Minimal machinery for membrane fusion. *Cell* **92,** 759–772.

Wen, C., Metzstein, M. M., and Greenwald, I. (1997). SUP-17, a *Caenorhabditis elegans* ADAM protein related to *Drosophila* KUZBANIAN, and its role in LIN-12/NOTCH signalling. *Development* **124,** 4759–4767.

White, J. (1988). The anatomy. *In* "The Nematode *Caenorhabditis elegans*" (W. B. Wood, Ed.), Chap. 4, pp. 81–122. Cold Spring Harbor Laboratory Press, Cold Spring Harbor, NY.

White, J. M. (1992). Membrane fusion. *Science* **258,** 917–923.

Wood, W. B. (1988). Introduction to *C. elegans* biology. *In* "The Nematode *Caenorhabditis elegans*" (W. B. Wood, Ed.), Chap. 1, pp. 1–16. Cold Spring Harbor Laboratory Press, Cold Spring Harbor, NY.

Wood, W. B. (1991). Evidence from reversal of handedness in *C. elegans* embryos for early cell interactions determining cell fates. *Nature* **349,** 536–538.

Received for publication September 23, 1998
Accepted November 17, 1998